Dissertations, Master's Theses and Master's Reports

2018

INVESTIGATION ON THE POTENTIAL OF A CO2 CAPTURE SYSTEM, DOWNSTREAM OF THE AFTERTREATMENT SYSTEM FOR A HEAVY-DUTY ENGINE APPLICATION

Murchana Pathak
Michigan Technological University, mpathak1@mtu.edu

www.manaraa.com

INVESTIGATION ON THE POTENTIAL OF A CO$_2$ CAPTURE SYSTEM,
DOWNSTREAM OF THE AFTERTREATMENT SYSTEM FOR A HEAVY-DUTY
ENGINE APPLICATION

By

Murchana Pathak

A THESIS

Submitted in partial fulfillment of the requirements for the degree of

MASTER OF SCIENCE

In Mechanical Engineering

MICHIGAN TECHNOLOGICAL UNIVERSITY

2018

© 2018 Murchana Pathak

This thesis has been approved in partial fulfillment of the requirements for the Degree of MASTER OF SCIENCE in Mechanical Engineering.

Department of Mechanical Engineering – Engineering Mechanics

Thesis Advisor: *Dr. Jeffrey D. Naber*

Thesis Co-Advisor: *Dr. Alexander K. Voice*

Committee Member: *Dr. Tom Tzanetakis*

Department Chair: *Dr. William Predebon*

Dedication

Mor poriyalor proti utsorgito

Table of Contents

v

List of figures

List of tables

Acknowledgements

I am sincerely thankful to Dr. Jeffrey D. Naber for his tremendous guidance throughout these two years. His patience and teaching, his dedication to learning and his continuous support and motivation has been a positive influence on my professional development. It has been a privilege to work under his mentorship and I am thankful to him for his direction throughout the research project.

I would like to thank Dr. Michael Traver and Dr. David Cleary of Aramco Research Center, Novi, MI for providing me the opportunity to work on this research project. My work has exposed me to a wide variety of topics and sciences and I have gained an immense amount of knowledge along the way.

I would like to thank my co-advisors and committee members, Dr. Alexander K. Voice and Dr. Tom Tzanetakis of Aramco Research Center, Novi, MI for their valuable time and incisive inputs to my research work. Dr. Voice's insights and expertise in the absorption-separation processes have been invaluable in guiding my work.

I would like to extend special thanks to Andy Noonan from Gamma Technologies LLC. He has been extremely helpful in solving issues with the GT model, answer my queries and doubts and helped me understand the heat exchanger design

concepts. Without his help, this would have been a lot more difficult and I appreciate his time and patience.

Finally, I wanted to thank my family, who has been my greatest support throughout this journey. My parents have always encouraged me to pursue whatever I choose and to do my best. I am and will always be eternally grateful to them for the opportunities and environment they have provided me. I also wanted to thank my friends for all their support and for making my experience as a graduate student much more enjoyable.

Abstract

The transportation sector accounts for the second largest source of CO_2 emissions after power generation. New Corporate Average Fuel Economy (CAFE) regulations are focusing on improving energy through reduced fuel consumption and greenhouse gas emissions. This work investigates the potential of a CO_2 capture system downstream of an aftertreatment system for a heavy-duty engine application. Amine absorption has been described as one of the most effective ways to capture CO_2 from exhaust for point sources. Therefore, using thermal-swing absorption process with potassium carbonate (K_2CO_3) as the absorbent liquid, a process was analyzed for onboard CO_2 capture with a 15-liter heavy-duty truck engine. The CO_2 capture system comprises of a CO_2 absorber that separates CO_2 from the exhaust; a CO_2 stripper or regenerator that regenerates the absorbent liquid; heat exchangers and coolers for maintaining the required temperature of the system; and a compressor for compressing the CO_2 for storage. The operating parameters of the CO_2 capture system, including liquid flow rates, lean/rich loading were estimated by assuming a driving force for the mass transfer. The regenerator pressure was determined from the vapor-liquid equilibrium data as a function of temperature and lean CO_2 loading. The components of the system were designed and simulated individually in GT-Suite at a 60% CO_2 capture rate and this allowed for determination of liquid flow rates, outlet temperature and the

heat transfer across the system for a mid-speed, mid-load operating condition. The components are then integrated in GT-Suite to form a CO_2 capture system model downstream of the aftertreatment system. The system performance was then determined for different exhaust gas conditions representative of the Supplemental Emissions Test (SET) operating conditions from idle to full load. The CO_2 capture requires both heat and power for the absorption as well as the separation process which can utilize the energy extracted from waste heat recovery system (WHRS). The exhaust heat would be used to heat the solvent and desorb the CO_2 in the stripper. Unlike point sources, the onboard CO_2 capture system has challenges such as space limitations and availability of processes and cooling water. However, exhaust heat also provides a low-cost source of waste heat not typically available at stationary power plants. This work aims to determine the heat duty, cooling duty, and compression work required for capturing CO_2 at different engine operating conditions.

Chapter 1

Introduction

The phenomenon of global warming, one of the direct results of climate change has raised concerns over the emission of greenhouse gases such as carbon dioxide (CO_2). As the world energy demand is increasing, greenhouse gas emissions are increasing, and this would require challenging efforts for reduction of CO_2 and other greenhouse gases in mitigating the climate change. A major source of CO_2 involves the combustion of fossil fuels. Among these various sources, coal-fired power generation is the largest contributor to CO_2 emission. Worldwide, the transportation sector accounts for 14% of all Greenhouse Gas (GHG) emissions and is therefore considered to be a significant source.

1.1. Motivation

Over the years, the Environmental Protection Agency (EPA) regulations for vehicular CO_2 emissions are becoming increasingly more stringent. New Corporate Average Fuel Economy (CAFE) regulations are focusing on improving energy efficiency through reduced fuel consumption and greenhouse gas

1

emissions. Although more sustainable transportation options like renewable energy and alternate fuels seem to be a solution to reduce CO_2 emissions, the extent to which these sources can be utilized is very limited and they cannot suffice the world energy requirement in the present or in the future. Electrification is another technology to reduce tailpipe carbon emissions and improve fuel consumption, but they rely primarily on CO_2 generating coal and gas fired power plants to charge the batteries. Also, cost and off-road utility are two major disadvantages of electric vehicles, and range and charge time are major challenges for electrification of the heavy-duty transportation industry.

1.2.Sources of GHG emissions

The worldwide greenhouse gas emissions resulting from the economic sector is shown in Figure 1.1 (EPA, 2016). Carbon dioxide emissions, being the most prominent source of greenhouse gas emissions, result from both natural and anthropogenic causes. Fossil fuel combustion is the primary source of CO_2 emissions which has increased steadily since the Industrial Revolution.

2

2015 Global Greenhouse Gas Emissions by Economic Sector

Other Energy 10%

Industry 21%

Transportation 14%

Buildings 6%

Electricity and Heat Production 25%

Agriculture, Forestry and Other Land Use 24%
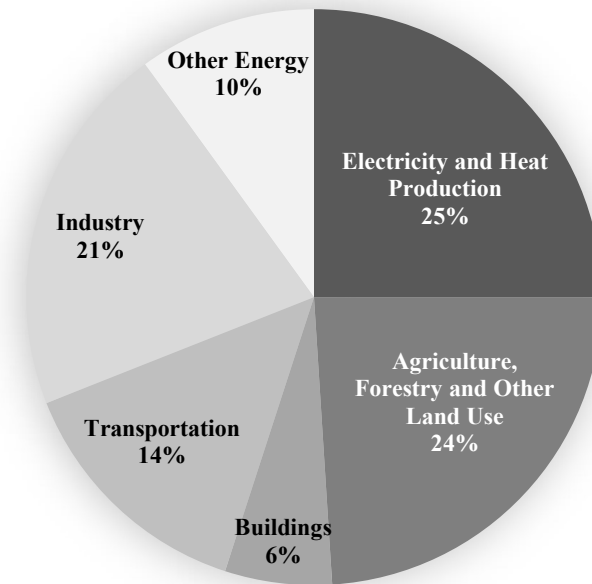
Figure 1.1. Worldwide GHG Emissions by Economic Sector in 2015, (EPA, 2016)

In 2015, fossil fuel combustion accounted for 93% of CO_2 emissions in the United States (EPA, 2015). The annual CO_2 emissions resulting from fossil fuel consumption from 1990 – 2015 are listed in Table 1.1 (EPA, 2015). From 1990 to 2015, the CO_2 emissions from the transportation sector in U.S. increased from 1493.8 million metric tons (MMT) CO_2 Eq. to 1736.4 million metric tons (MMT) CO_2 Eq., a 16.2 percent total increase over the twenty-six-year period.

Table 1.1. CO$_2$ Emissions from Fossil Fuel Combustion by End-Use Sector (MMT CO$_2$ Eq.)

Gas/Source	1990	2000	2010	2011	2012	2013	2014	2015
Fossil Fuel Combustion	**4740.3**	**5593.7**	**5359.4**	**5227.1**	**5024.6**	**5156.5**	**5202.3**	**5049.8**
Electricity Generation	1820.8	2296.9	2258.4	2157.7	2022.2	2038.1	2038	1900.7
Transportation	1493.8	1805.5	1728.3	1707.6	1696.8	1713	1742.8	1736.4
Industrial	842.5	854.1	775.5	775	782.9	812.2	806.1	805.5
Residential & Commercial	555.7	601.7	554.7	545.9	479.2	550.7	574.1	565.8

Figure 1.2 illustrates the five-major fuel consuming economic sectors contributing to CO$_2$ emissions from fossil fuel and non-fossil fuel combustion. Electricity generators produce 36% while transportation activities account for 32% of U.S. CO$_2$ emissions from fossil fuel consumption in 2015 (EPA, 2015). Medium and heavy-duty trucks account for 23% of CO$_2$ emissions, most of which consume around 2.7 million barrels of fuel, emitting a total of 530 million metric tons of CO$_2$. Industrial emissions result from both fossil fuel consumption and electricity

4

www.manaraa.com

generation while residential and commercial sectors rely heavily on electricity. Other sources or non-fossil fuel combustion includes CO_2 emissions from nuclear energy, hydroelectric energy or geothermal energy.

2015 U.S. Carbon Dioxide Emissions
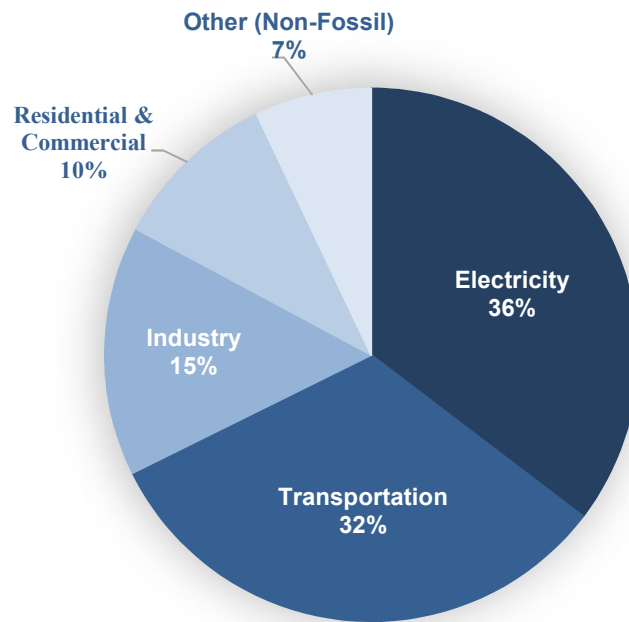
Figure 1.2. U.S. CO_2 Emissions from Fuel Combustion in 2015, (U.S. EPA, 2017)

1.2.1. The Greenhouse Effect

The solar radiations from the sun are converted to infrared radiations or heat when they reach the earth surface. A part of these radiations or heat is absorbed by the gases in the earth's atmosphere and are re-radiated back to the earth. This phenomenon is called the greenhouse effect and the gases on earth's atmosphere responsible for this phenomenon are called greenhouse gases.

5

Carbon dioxide (CO_2) is the most predominant greenhouse gas followed by water vapor, ozone (O_3), methane (CH_4), Nitrous oxide (N_2O), etc. From 1990 to 2015, the total greenhouse gas emissions have increased by an overall 3.5%. In 2015, the U.S. gross greenhouse emissions were 6586.7 MMT of CO_2 Eq. out of which CO_2 emissions accounted for 5411.4 MMT of CO_2 Eq. Figure 1.3 shows the contribution of greenhouse gases to the total emissions in the U.S. in 2015. CO_2 is the primary greenhouse gas that resulted in 82% of the total emissions followed by methane (CH_4) which contributes around 10%. Fossil fuel combustion was the major source of CO_2 emissions as well as overall greenhouse gas emissions. Nitrous Oxide (N_2O) and other fluorinated gases like hydrofluorocarbon (HFC), perfluorocarbon (PFC), Sulphur hexafluoride (SF_6) and Nitrogen trifluoride (NF_3) contributed around 5% and 3% of the total emissions respectively.

2015 U.S. Greenhouse Gas Emissions

Nitrous Oxide 5%

Fluorinated Gases 3%

Methane 10%

Carbon Dioxide 82%
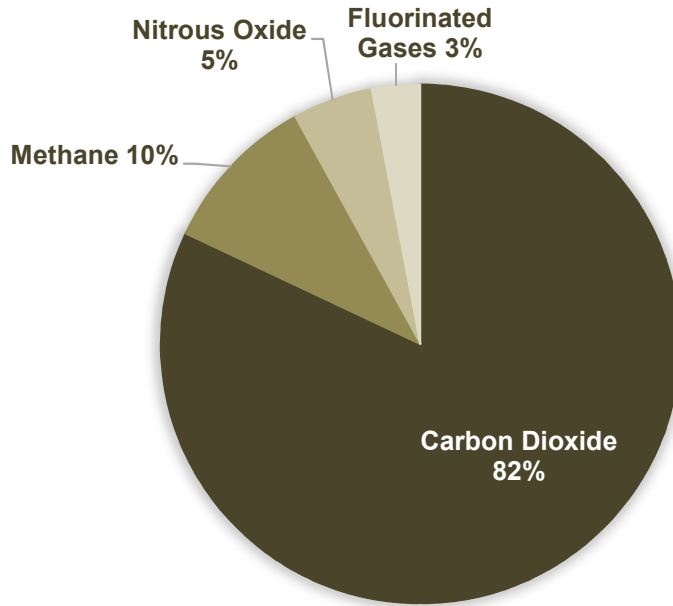
Figure 1.3. U.S. Greenhouse Gas Emissions in 2015 by gas source (U.S EPA, 2017)

1.2.2. Atmospheric CO_2 levels

Before the Industrial Revolution, the amount of CO_2 in the atmosphere was 280 parts per million (ppm). Since then, the rate of CO_2 has been increasing at an alarming rate and has reached a level of 406.56 parts per million by June 2017 according to National Oceanic and Atmospheric Administration (NOAA) researchers. Figure 1.4 depicts the monthly average atmospheric CO_2 levels measured at Mauna Loa Observatory in Hawaii with average seasonal cycle removed. Most of the atmospheric CO_2 is through a natural process. But human caused, or anthropogenic CO_2 makes its way into the atmosphere through different

paths. Energy-related activities are the largest anthropogenic contributor to CO_2 emissions, a wide majority of which accounts for combustion of fossil fuels followed by deforestation. There is a natural balance of carbon dioxide in the atmosphere and ocean as the carbon dioxide in the atmosphere is absorbed by the ocean and that in ocean rises to the atmosphere. However, the ocean is unable to absorb a large amount of carbon dioxide produced by the anthropogenic causes and this results in an increase of CO_2 levels in the atmosphere.
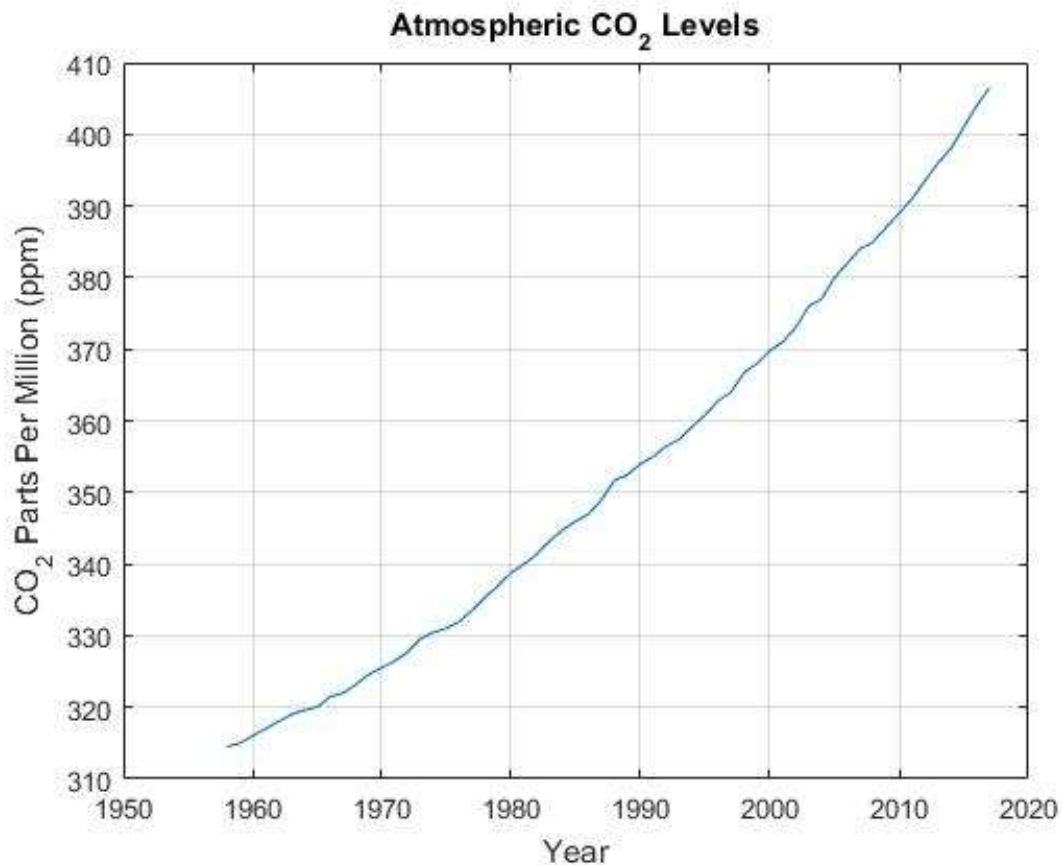
Figure 1.4. Monthly mean Atmospheric CO_2 levels from 1958 – 2017

(NOAA/ESRL, 2017)

8

1.3.Remediation of Carbon Dioxide

To prevent the atmospheric CO_2 content from increasing at a rapid rate, the anthropogenic causes of CO_2 emissions must be curbed. Decreasing the rate of CO_2 emissions produced by burning fossil fuels is critical to that effort. Consumption of petroleum as a transportation fuel has been the largest CO_2 emission contributor in the post-industrial era.

1.4.Absorption/ Stripping Process

Absorption is the mass transfer of a substance from the gaseous phase to the liquid phase. The substance absorbed can be bound by the liquid both physically and chemically. Amine solutions used in gas treating technology react reversibly with dissolved CO_2. This has been established as one of the most effective ways to capture CO_2 from exhaust gas for point sources. The most common absorption process utilizes the concept of thermal swing absorption with a circulated chemical solvent. So, a process was analyzed for an onboard CO_2 capture system with a 15-liter heavy-duty truck engine. The exhaust gas going through the absorber is counter-currently brought in contact with an amine solvent at a low temperature. CO_2 from exhaust gas then reacts with the solvent with exothermal chemical reactions thereby reducing the concentration of CO_2 gas from the stream exiting the absorber. The solvent stream with a higher concentration or rich loading of CO_2 goes through a cross exchanger where it is heated up to a high temperature before it enters the stripper. The temperature of the stripper is

9

maintained at a high temperature so that absorption process is reversed, and the solvent stream liberates the CO_2. The solvent stream with a lower concentration or lean loading of CO_2 passes through the cross exchanger where its temperature is reduced and is sent to the absorber to absorb more CO_2 from the incoming exhaust gas stream.

1.4.1. Solvents

A great variety of solvents can be used for exhaust gas treating but the most effective solvents considered for CO_2 removal are aqueous amines or hot potassium carbonate (K_2CO_3). 30% wt. 7m monoethanolamine or MEA is one of the most widely used amine solvents in CO_2 removal from flue gas because of its faster absorption rate but its performance is limited by its maximum operating temperature, rate of CO_2 absorption, cyclic CO_2 capacity, corrosion issues as well as oxidative and thermal degradation. Despite having poor thermodynamic properties, potassium carbonate has the advantage of being non-volatile and not subject to degradation – properties which are advantageous for onboard applications. Furthermore, its poor heat of absorption can potentially be compensated for by operating the stripper at much higher temperature using waste exhaust heat. The choice of solvent influences the energy requirements, cooling requirements, and equipment size for the CO_2 capture system and is, therefore, an important factor to consider for optimizing energy flow along with the absorption rate.

10

1.4.2. Energy requirement and technical challenges

The CO_2 capture system requires a considerable amount of energy for solvent regeneration and compression of CO_2. In addition to that, energy is required for the heat exchanger, coolers, and condenser required to maintain the temperature of the system. For a heavy-duty engine, the integration of the CO_2 capture system to a waste heat recovery system following the exhaust gas recirculation (EGR) and downstream of the aftertreatment system, can reduce the energy penalty of the process. The waste heat recovery system utilizes the concept of an Organic Rankine cycle (ORC) with a working fluid to harvest energy from the engine's heat dissipating circuits. The energy recovered could be used to provide power for compression of CO_2 in the separation process while the remaining exhaust heat could be utilized in solvent regeneration and desorption of CO_2 in the stripper. Calorimetry affects the sizing of heat exchangers which in turn affects the energy requirements for solvent regeneration. The temperature of the engine's exhaust gas is very high and is required to be brought down by a considerable amount before it goes through the absorber owing to the thermal swing variation. However, exhaust heat also provides a low-cost source of waste heat not typically available at stationary power plants. The gas rate, CO2 concentration, liquid rate, and lean loading all play an important role in determining the design specifications for height and diameter of the CO_2 absorber system. Other technical challenges involve CO_2 storage, collection, transportation, and disposal. The CO_2 collected can be stored onboard the vehicle temporarily before

11

being offloaded during refueling. Transportation to the disposal site can occur through existing CO_2 pipelines and injected into suitable deep rock geological formations underground for long term storage in depleted oil and gas reservoirs or to recover oil. Subsurface geological storage of CO_2 both onshore and offshore along with CO_2 capture can cut down emissions (IPCC, 2005).

1.5. Scope of work

The focus of this work is to –

1. Determine the energy requirement for absorption and desorption of CO_2 for a heavy-duty engine application at a mid-speed, mid-load operating condition.

2. Study the solvent properties required for the absorption process.

3. Design a solvent regenerator model to obtain the CO_2 VLE data and evaluate the solvent parameters throughout the system.

4. Design a CO_2 capture system in GT-Suite for an on-board application to evaluate the energy requirements and solvent parameters for different operating conditions.

1.6. Outline of the thesis

The thesis is organized into five chapters. Chapter 1 gives a brief overview of the objective and motivation behind the work, the fundamentals of the CO_2 absorption process and its challenges in an on-board system. Chapter 2 provides an overview on the theories of mass transfer with chemical reactions, equilibrium

12

and solvent rate behavior for a deeper understanding of the absorption process. Chapter 3 defines the CO_2 capture system and its components for a heavy-duty application including the assumptions, boundary conditions and steps to calculate their individual performance. A model is developed in GT-Suite® to simulate the energy transfer across the system as well as solvent parameters for all the SET operating conditions from idle to full load. Chapter 4 discusses the results obtained from the VLE data, the solvent properties and the CO_2 loading throughout the system as well as the heat transfer rate and flow rates for different operating conditions obtained from the GT model. Chapter 5 summarizes the overall methodology and results from this work and provides recommendations to further expand this research.

Chapter 2

Literature Review

This chapter presents the relevant theories and literature pertaining to the study of CO_2 absorption by aqueous amines and other solvents for point sources. A brief theory on the mass transfer with chemical reactions as well as equilibrium and rate behavior of solvents with an emphasis on potassium carbonate is discussed in this chapter with related assumptions and boundary conditions.

2.1. Mass Transfer Theory

The mass transfer of CO_2 from the exhaust gas to a liquid involves diffusion in both liquid and gas phase, physical solubility at gas-liquid interface and chemical reactions in the liquid. The role of diffusion and chemical reactions in the liquid is the most complicated part of the mass transfer process in the liquid phase. The properties of the solvent have a significant influence on the mass transfer of CO_2 in liquid thereby making the basics of mass transfer theories in the liquid phase a vital element for choosing the best solvent [3].

14

2.1.1. Mass Transfer Coefficients

The gas molecules diffuse in the liquid in the process of physical absorption. The flux, N_{CO2} represents the rate of mass transfer at unit area and can be calculated at the gas-liquid interface ($x = 0$) as –

$$N_{CO_2} = -D_{CO_2} \frac{\partial [CO_2]}{\partial x}\bigg|_{X=0} \qquad (2.1)$$

The flux is proportional to the concentration driving force for mass transfer across the boundary layers. In case of CO_2 absorption from gas to liquid, flux can be calculated for driving force in both gas and liquid film and is same at any point within the boundary layer. The proportionality constant between flux and its corresponding driving force is the mass transfer coefficient.

$$N_{CO_2} = \begin{cases} K_G\left(P_{CO_2} - P_{CO_2}^*\right) \\ k_g\left(P_{CO_2} - P_{CO_2,i}\right) \\ k_l\left([CO_2]_i - [CO_2]\right) \\ k_g'\left(P_{CO_2,i} - P_{CO_2}^*\right) = \frac{k_l}{H_{CO_2}}\left(P_{CO_2,i} - P_{CO_2}^*\right) \end{cases} \qquad (2.2)$$

Where K_G represents the overall gas phase mass transfer coefficient, k_g is the gas phase mass transfer coefficient and k_l is the liquid phase mass transfer coefficient and k_g' is the liquid phase mass transfer coefficient defined in gas phase units. P_{CO2} indicates the bulk gas partial pressure of CO_2, P_{CO2}^* is the equilibrium partial pressure of CO_2 in the bulk liquid and $P_{CO2,i}$ is the partial pressure of CO_2 at gas-liquid interface. K_G corresponds to the concentration driving force between

15

bulk gas and bulk liquid where $P^*_{CO_2}$ is in equilibrium with $[CO_2]$. k_g and k_l correspond to driving force across the gas film and liquid film respectively. Both k_l and k'_g are functions of liquid properties. H_{CO_2} is the Henry's constant of CO_2 in the solvent and is used to denote the equilibrium of CO_2 in the gas and liquid at the gas-liquid interface [3].
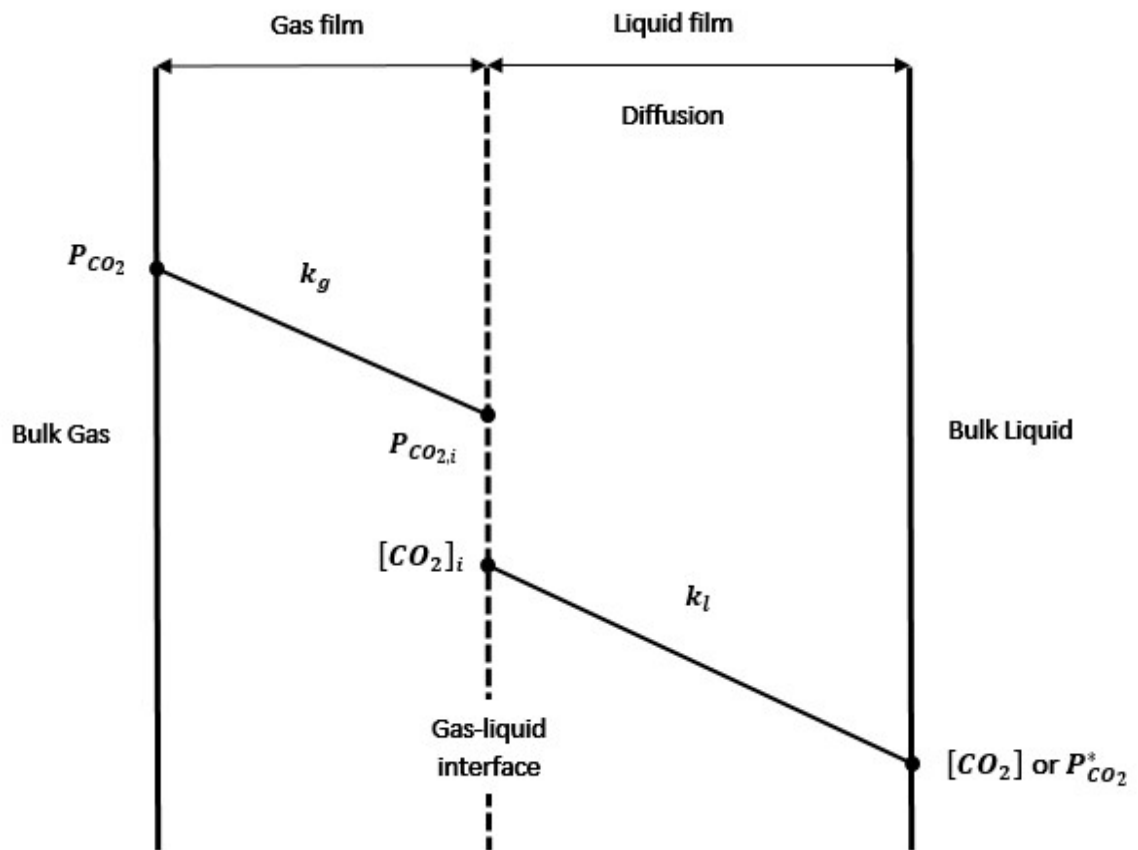
Figure 2.1. Schematic of Physical Mass Transfer of CO_2 into Bulk Liquid

CO$_2$ molecules from the gas phase move to the gas-liquid interface where it dissolves. The dissolved CO$_2$ then reacts with the solvent, diminishes from the interface and diffuses into the bulk liquid.

16

The flux in Equation 2.2 is constant and can be combined to represent addition of series resistances to mass transfer. The overall mass transfer coefficient in a physical absorption is same as the sum of gas film and liquid film mass transfer coefficients.

$$\frac{1}{K_G} = \frac{1}{k_g} + \frac{H_{CO_2}}{k_l} = \frac{1}{k_g} + \frac{1}{k_g'} \qquad (2.3)$$

In a chemical reaction, most of the reactions occurs in the Reaction film, which is a thin layer between the gas-liquid interface and the reaction-diffusion interface as shown in Figure 2.2. The chemical reaction monitors the equilibrium at the interface and the driving force is represented by equilibrium and diffusion of CO_2 into the reaction film for reversible reactions. The series resistance relationship can be expressed as –

$$\frac{1}{K_G} = \frac{1}{k_g} + \frac{1}{k_g''} + \frac{1}{k_{l,PROD}} \frac{\partial P_{CO_2}^*}{\partial [CO_2]_T} \qquad (2.4)$$

Since k_g comprises of both reaction and liquid diffusion films, it has both reaction and diffusion component which is shown in Equation 2.4. The term k_g'' is the pseudo first order term denoting the reaction kinetics of the solvent. The third term in the Equation 2.4 represents diffusion resistance where $\partial P_{CO_2}^*/\partial [CO_2]_T$ denotes the slope of the equilibrium line. It enables a series resistance relationship by changing the CO_2 concentration driving force to partial pressure driving force [8].

17
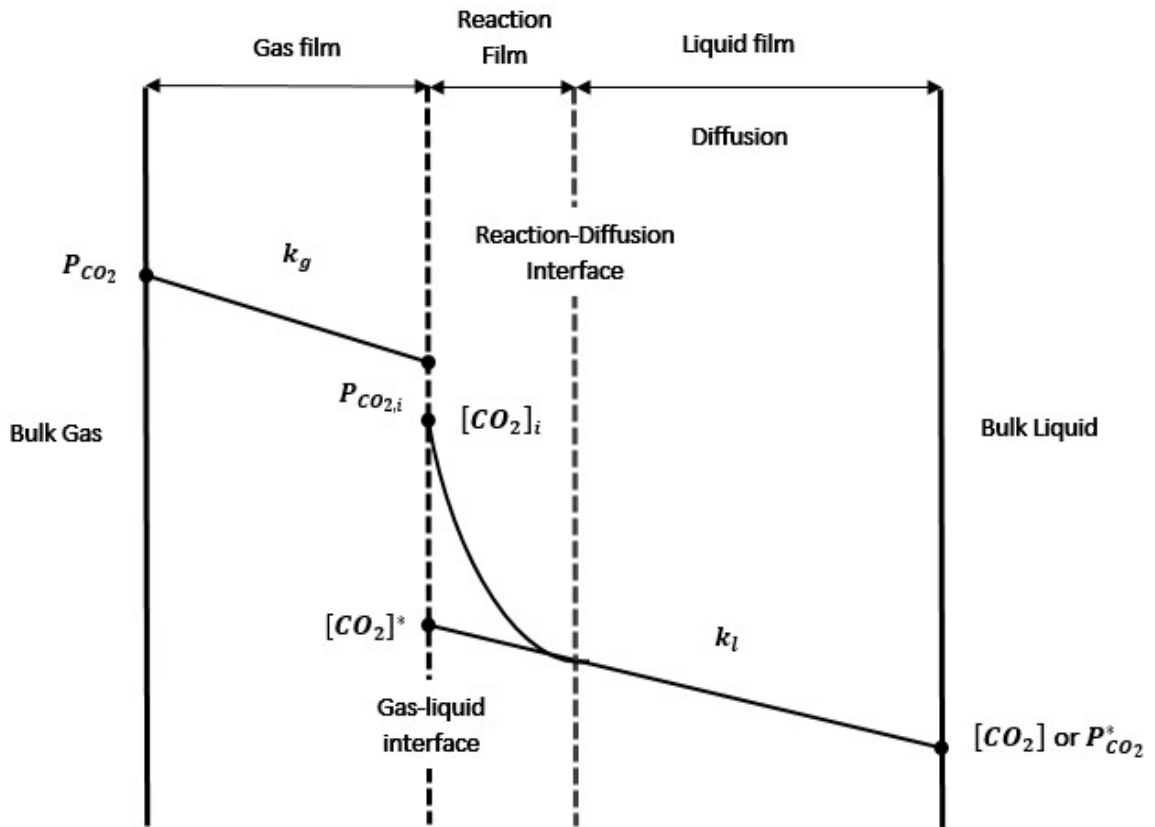
Figure 2.2. Schematic of Mass Transfer of CO_2 into Bulk Liquid with Fast

Chemical Reaction

As shown in Figure 2.2, the system includes resistance for gas film, reaction film and liquid diffusion film. If the reaction film resistance is predominant in a system while the liquid diffusion resistance is negligible it leads to a pseudo first order reaction. If the liquid diffusion film resistance is predominant and the reaction resistance is negligible the system leads to an instantaneous reaction condition.

18

2.2. Pseudo First Order Reaction

The pseudo first order reaction is an approximation that simplifies mass transfer with fast chemical reaction. It assumes that the concentration of amine in the solvent for reacting with CO_2 is higher relative to CO_2 flux. Applying the pseudo first order assumption, the rate of CO_2 reaction can be expressed as –

$$D_{CO_2} \frac{\partial^2 [CO_2]}{\partial x^2} - k_2 [Am][CO_2] = 0 \qquad (2.5)$$

Assuming both the amine concentration and the solvent concentration are same at the bulk liquid interface,

$$D_{CO_2} \frac{\partial^2 [CO_2]}{\partial x^2} - k_2 [Am]_b [CO_2] = 0 \qquad (2.6)$$

where $[Am]_b$ is the amine concentration with bulk solution composition. Using boundary conditions and neglecting the physical absorption of CO_2, the flux is represented for reversible reactions as follows –

$$N_{CO_2} = \frac{\sqrt{D_{CO_2} k_2 [Am]_b}}{H_{CO_2}} \left(P_{CO_{2,i}} - P_{CO_2}^* \right) \qquad (2.7)$$

From pseudo first order concentrations, the flux is expressed as –

$$k_g = \frac{\sqrt{D_{CO_2} k_2 [Am]_b}}{H_{CO_2}} \qquad (2.8)$$

19

2.3. Instantaneous Reaction

The instantaneous reactions involve mass transfer with chemical reactions that are very fast or instantaneous with respect to diffusion. These reactions usually occur at high temperatures with increase in kinetics or low solvent concentrations. The mass transfer is driven by the diffusion of reactants from reaction film and the diffusion of products from the reaction film. The total solubility of CO_2 is represented by all dissolved forms like carbamate and bicarbonate of gas and the mass transfer rate is expressed as –

$$N_{CO_2} = k_l\big([CO_2]_{i,T} - [CO_2]_T^*\big) = k_l\left(\frac{P_g}{H_{CO_2}} - [CO_2]_T^*\right) \qquad (2.9)$$

Where $[CO_2]_{i,T}$ is the total concentration of the dissolved CO_2 at gas-liquid interface, P_g is the CO_2 partial pressure in gas phase and in equilibrium with the dissolved CO_2 at gas-liquid interface and H_{CO_2} is the Henry's constant of CO_2 in the solvent.

An instantaneous reaction case could be seen at the CO_2 stripper conditions. The stripper operates at a high temperature and thereby has higher driving forces of CO_2 partial pressure. The high partial pressure driving forces rule out the role of kinetics hence making the liquid phase diffusion coefficients the only factors contributing to the mass transfer.

20

2.4. Solvents for CO₂ absorption

This discussion includes the basic thermodynamic and chemical analysis of different types of solvents used for CO_2 absorption.

2.4.1. Amines

Amines are organic compounds containing a basic nitrogen atom. Based on their structure, amines are subdivided as primary and secondary amines, tertiary amines and hindered amines. Primary amines have one carbon atom connected to the nitrogen while secondary amines have two carbon atoms. They have open structures that enables CO_2 to form carbamates with the nitrogen. Tertiary amines have three carbon atoms attached to the nitrogen which makes it unstable for carbamates and forms bicarbonates instead. Hindered amines are primary and secondary amines with functional groups around the nitrogen that can hinder the formation of stable carbamates (Satori and Savage 1983). They can react with CO_2 to form carbamates at a lower equilibrium concentration. Hindered amines can convert CO_2 to bicarbonate with water like tertiary amines and have higher solvent capacity than primary and secondary amines.

A significant amount of literature data on rate studies of amines is available of which most of the studies are concerned with reactions of MEA and CO_2. Previous work on amines with CO_2 have been done by Dugas (2009) with 7-13 m MEA; Chen (2011) with 10 m Diglycolamine (DEA), 8 m 1,2-Diaminopropane (MEDA), 8

21

m 1 & 2 Methylpiperazine; Bishnoi (2000) with 7.6 m Methyldiethanolamine (MDEA) with Piperazine (PZ), focusing on absorption rate and capacity.

2.4.2. Potassium Carbonate

Potassium Carbonate (K_2CO_3) has been used for CO_2 absorption in natural gas treating and ammonia production for a long time. In 1954 and 1956, Benson *et al.* studied the pilot plant characterization of hot potassium carbonate and MEA, validating the use of K_2CO_3 as an effective CO_2 absorbent in the commercial market and utilized it for treating synthesis gas in 1959.

The absorption of CO_2 into K_2CO_3 is represented by the following overall reaction –

$$CO_3^{2-} + CO_2 + H_2O(aq) \leftrightarrow 2HCO_3^- \qquad (2.10)$$
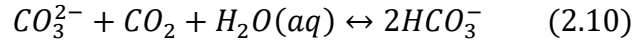
Which can also be expressed as two parallel reversible reactions

$$CO_2(aq) + OH^- \leftrightarrow HCO_3^- \qquad (2.11)$$

$$HCO_3^- + OH^- \leftrightarrow CO_3^{2-} + H_2O \qquad (2.12)$$
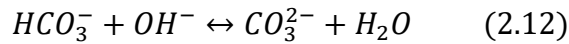
The reaction rate is represented as a second order rate expression.

$$r_{CO_2} = k_{OH^-}[OH^-][CO_2] \qquad (2.13)$$

The reaction is usually slower than aqueous amines, but the energy required to reverse the reaction is lesser than that for amine solvents. However,

this low heat of absorption also means that at a given temperature, CO_2 is produced at a lower pressure, increasing the amount of water vaporized per mol of CO_2 as well as the compression work. Lastly, potassium carbonate is non-volatile and not prone to degradation reactions and hence there is no solvent loss due to degradation.

2.5. CO_2 Loading

The CO_2 loading represents the CO_2 concentration in a solution. It is given by the ratio of CO_2 molecules to the equivalent alkalinity. The CO_2 loading is expressed mathematically as –

$$CO_2 \ Loading = \frac{n_{CO_2}}{n_{solvent}} \qquad (2.14)$$

n_{CO_2} and $n_{solvent}$ represents the number of moles of CO_2 and the solvent respectively. In some cases, loading is expressed as per mole of basicity rather than per mole of solvent, thus the definition can depend on the solvent in question. The CO_2 loading for potassium carbonate solution can be represented by –

$$CO_2 \ Loading = \frac{n_{CO_2}}{n_{K_2CO_3}} \qquad (2.15)$$

23

Chapter 3

System Definition and Model Development

This chapter includes the development of the CO_2 capture system, its assumptions and thermodynamic considerations as well as the model integration for a heavy-duty truck engine.

3.1. CO_2 Capture System

The CO_2 capture system utilizes the thermal swing absorption process with a circulated chemical solvent. A schematic of the CO_2 capture system is developed for an on-board application as shown in Figure 3.1. The exhaust gas coming out of the Selective Catalytic Reduction (SCR) of the aftertreatment system at temperature T_1 is sent through an exhaust heat exchanger where its temperature reduces to T_2. The exhaust gas with low temperature T_2 passes through the absorber before it exits via the tailpipe. The absorbent liquid or solvent is sent through the absorber in a counter-current direction where it absorbs the CO_2 from the exhaust gas at low temperature. The absorbent liquid now rich with CO_2 loading is sent to the absorbent-absorbent heat exchanger and the exhaust

24

absorbent heat exchanger where its temperature is increased to T_5 before it enters the stripper. At high temperature of T_4, the CO_2 molecules are released from the absorbent liquid molecules producing a CO_2-lean absorbent solution leaving the stripper. The absorbent then circulates back through the absorbent-absorbent heat exchanger and trim cooler that brings its temperature down to T_2 before it returns to the absorber. The CO_2 stream from the stripper is then sent through a condenser where it is condensed to T_6 and the water is collected. The CO_2 is then sent to the compressor where it is compressed to P_3 before it goes to the storage tank.
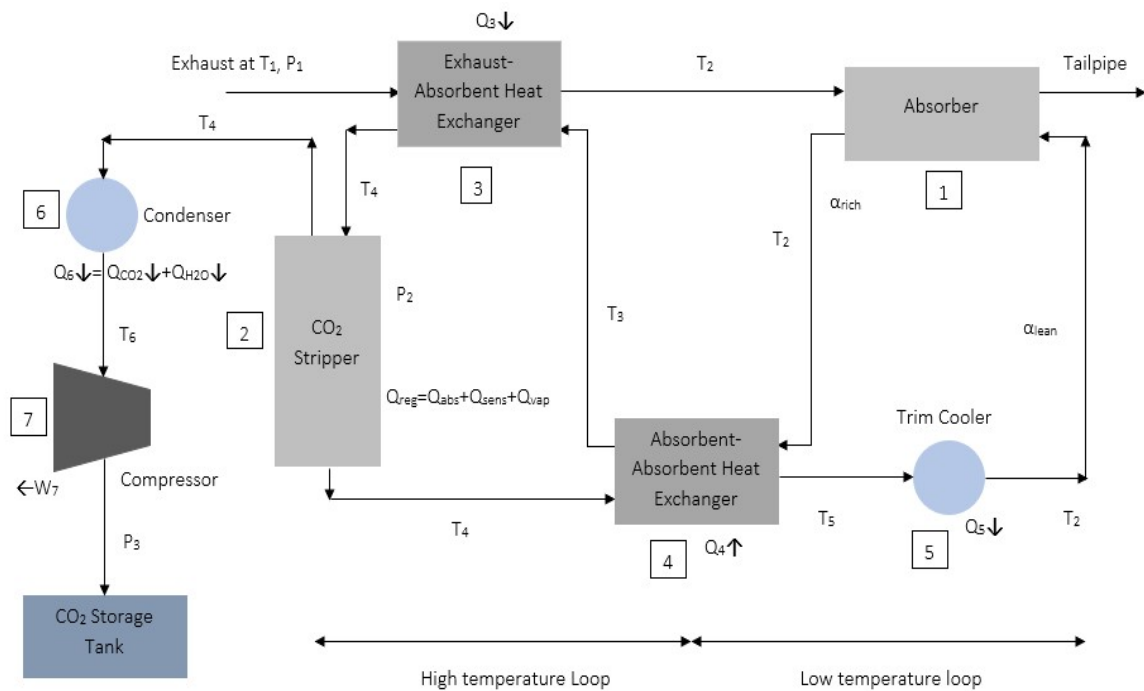
Figure 3.1. Schematic of the on-board CO_2 Capture system

25

3.2. Sub-components of the system

3.2.1. Absorber

The absorber usually consists of one or more membrane contractors, which comprises of a bundle of narrow porous tubes encompassed by a cylindrical shell. The solvent flows through these tubes while the exhaust flows through the shell outside the tubes. The solvent absorbs the CO_2 from the exhaust gas through the porous tubes before the exhaust gas leaves the tailpipe. The exhaust gas and the solvent must be brought down to a low temperature of 40-60°C before it is sent through the absorber. This is important, as at higher temperatures, the CO_2 molecules would break away from the solvent molecules thereby making the absorption process less effective.
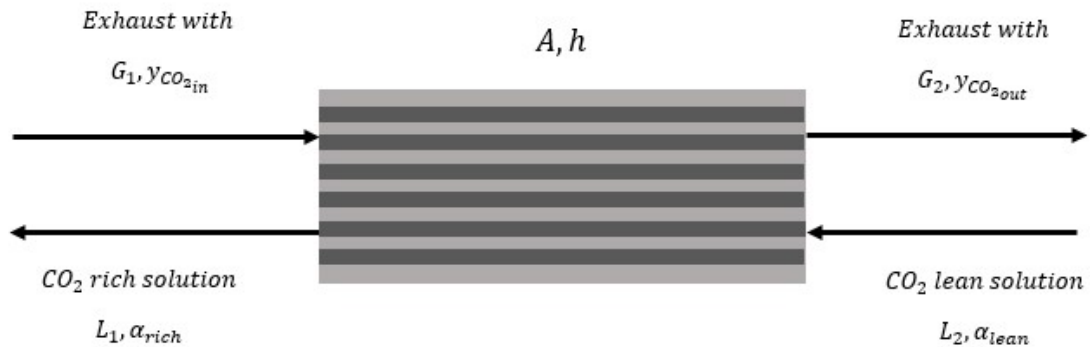
Figure 3.2. Functional diagram of an absorber

Where G_1 is exhaust gas flow rate with CO_2 composition $y_{CO_{2_{in}}}$ entering the absorber and G_2 is exhaust gas flow rate with CO_2 composition $y_{CO_{2_{out}}}$ leaving the absorber. L_2 and L_1 are solvent or liquid flow rates entering and leaving the absorber. α_{lean} and α_{rich} are the CO_2 lean loading and rich loading respectively.

The mass balance in the absorber is given by the following equation

$$G_1 y_1 + L_2 x_2 = G_2 y_2 + L_1 x_1 \qquad (3.1)$$

Where x_2 and x_1 are the moles of CO_2 per mole of solvent for lean loading and rich loading. y_1 and y_2 are mole fraction of CO_2 in the exhaust gas entering and leaving the absorber respectively.

The mole fraction of CO_2 in the liquid stream is given by –

$$x_{CO_2} = \frac{No.\ of\ moles\ of\ CO_2\ in\ the\ stream}{Total\ no.\ of\ moles\ in\ the\ stream} \qquad (3.2)$$

$$n_{K_2CO_3} = \frac{wt\%_{K_2CO_3}\ x\ 100gm}{MW_{K_2CO_3}} \qquad (3.3)$$

$$n_{H_2O} = \frac{wt\%_{H_2O}\ x\ 100gm}{MW_{H_2O}} \qquad (3.4)$$

$$n_{CO_2} = n_{K_2CO_3} * Loading \qquad (3.5)$$

Where n_i is the no. of moles of component i, MW_i is the molecular weight of component i, wt.%$_i$ is the percent weight fraction of component i, x_i is the mole fraction of the component i and 100gm is assumed as the basis for the solution.

The CO_2 absorption rate or capture rate of the absorber is represented as –

$$CO_2 \ Capture \ rate(\%) = \frac{amount \ of \ CO_2 \ captured}{amount \ of \ CO_2 \ entering} 100(\%) \qquad (3.6)$$

From Table 1, we can obtain the exhaust flow rate, G_1 and the amount of CO_2, y_1 in the exhaust stream. Hence, the molar flow rate of CO_2 entering the absorber can be calculated by the following equation.

$$n_1 = y_1 G_1 \qquad (3.7)$$

Assuming a CO_2 capture rate of 60%, the molar flow rate of CO_2 in the exhaust stream leaving the absorber can be calculated using the following equation.

$$CO_2 \ Capture \ rate(\%) = \frac{n_1 - n_2}{n_1} 100(\%) \qquad (3.8)$$

With the newly obtained value of n_2, the exhaust flow rate leaving the absorber, G_2 can be determined by using the following equation.

$$G_2 = G_1 - n_1 + n_2 \qquad (3.9)$$

Hence, the CO_2 composition in the exhaust stream leaving the absorber, y_2 can be determined by the following equation.

28

$$y_2 = \frac{n_2}{G_2} \qquad (3.10)$$

The amount of CO_2 removed from the exhaust stream in the absorber is modelled physically in GT-Suite® using an EjectorConn™ template. The EjectorConn™ extracts the calculated amount of CO_2 from the exhaust stream for the 13 SET operating points. The input parameters of EjectorConn™ requires the ejection rate of CO_2 from the exhaust stream. An absorber model using Radfrac™ template is designed in Aspen Plus with exhaust parameters of B50 operating point as the input which gives a capture efficiency of 64%. Hence, assuming a CO_2 capture rate of 60% for B50 point, the amount of CO_2 captured is calculated using equations 3.6 – 3.10 for all the SET operating points. The rate of CO_2 captured is then added to the solvent stream using an InjRateConn™ template. The input parameters of the InjRateConn™ are the rate of CO_2 captured and the temperature of the CO_2 stream. The temperature of the CO_2 stream is kept at 40°C since the absorption process is assumed to operate at 40°C.

A CO_2 Injector template is used in GT-Suite® to add the CO_2 removed from exhaust gas to the solvent stream. The CO_2 flow rate and the temperature at which it is injected are provided as input. The CO_2 flow rate can be calculated from the exhaust gas flow rate and CO_2 capture rate.

3.2.1.1. Exhaust gas parameters

The engine operating condition determines the flow rate, CO_2 composition, temperature and pressure of the exhaust gas. In this work, the system was designed based on the exhaust conditions at the "B50" operating point that represents a mid-load, mid-speed condition from the Supplemental Emissions Test (SET) data of a Cummins ISX15 engine with aftertreatment system. The operating points representing the exhaust parameters from idle to full-load conditions in the engine map are listed in Table 3.1.

Table 3.1. Exhaust gas parameters for the SET operating points

SET Points	Temperature (°C), T_1	Flow rate (kg/hr), G_1 or $\dot{m}_{exhaust}$	CO_2 Composition (%), y_1	Pressure (kPa), P_1
A25	322.8	412.62	7.45	3.19
A50	380.4	626.28	9.17	5.73
A75	419.8	832.68	10.12	9.13
A100	429.6	1117.14	10.18	13.5
B25	337.9	496.92	7.46	3.99
B50	354.4	811.44	8.33	7.6

B75	378.5	1089.9	9.09	11.98
B100	406.1	1405.5	9.48	17.83
C25	331.8	586.68	7.05	4.98
C50	336.8	922.8	7.89	8.95
C75	368.8	1203.42	8.76	13.35
C100	412.2	1477.92	9.36	19.24
Idle	193	154.14	2.35	0.15

An EndFlowInlet™ template in GT Library labelled as EndFlowInlet-Exhaust-in is used to provide the input parameters of the exhaust gas as shown in Table 3.1 in the GT model.

3.2.1.2. Absorbent liquid or Solvent

The absorbent liquid or solvent chosen for CO_2 absorption studied in this work was potassium carbonate (K_2CO_3) solution due to its non-volatility and negligible solvent losses associated with degradation. High potassium carbonate concentration is preferable due to increased CO_2 carrying capacity, however solvent viscosity and solid precipitation impose limits on the maximum practical concentration. According to the studies performed by Benson et. al. (1954) for a

31

K_2CO_3 system, it was found that at 50 and 60 wt.% solution, the precipitation occurs around their respective boiling points before the bicarbonate conversion exceeds 50%. But, in case of 40 wt% solution, the precipitation doesn't occur at its boiling point until bicarbonate conversion of 90%. Hence, the solvent used in this work is 40 wt% K_2CO_3 solution which is also the preferred expression for most gas treatments.

3.2.1.3. Solvent or liquid rate selection

The absorber performance for a given gas flow rate and CO_2 concentration depends on the dimensions of the absorber, the flow rate of the solvent, and the inlet CO_2 concentration (or lean loading) of the solvent. A solvent with a low flow rate loads up quickly decreasing the absorption rate. Although a lower lean loading can keep the CO_2 absorption rate constant, it requires a considerably large amount of energy to regenerate the solvent at the stripper. At a higher solvent flow rate, the amount of CO_2 removal can be constant with higher lean loading while reducing the energy for solvent regeneration. However, very high solvent rates lead to a higher sensible heat and increases the loading from the solvent feed to the stripper thereby affecting its vapor-liquid equilibrium. For a given exhaust CO_2 capture rate, an optimum solvent rate and lean loading can be determined.

3.2.1.4. Vapor-Liquid Equilibrium

The vapor-liquid equilibrium (VLE) of CO_2 in aqueous K_2CO_3 is affected by the physical solubility of gaseous CO_2 in the solvent and the chemical equilibrium

32

between the CO_2 dissolved and the other species in the solvent. The physical solubility of gaseous CO_2 in the solvent is expressed using Henry's law.

$$P^*_{CO_2} = H_{CO_2-solvent}x_{CO_2} = H_{CO_2-water}x_{CO_2}y_{CO_2} \qquad (3.11)$$

The dissolved CO_2 is in chemical equilibrium with the K_2CO_3 products and CO_2 products. The total CO_2 in the liquid phase is the sum of the dissolved CO_2 and the other species containing CO_2 products.

$$[CO_2]_T = [CO_2] + [CO_3^{2-}] + [HCO_3^-] \qquad (3.12)$$

The $[CO_2]$ in liquid phase is very low at most conditions due to the strong effect of the chemical reactions. So, in most CO_2 VLE representations, $[CO_2]_T$ is used instead of CO_2.

3.2.1.5. Cyclic Capacity

The CO_2 carrying capacity, or the cyclic capacity is the difference in CO_2 concentration between rich and lean CO_2 loading. It is expressed as the amount of CO_2 removed per unit mass of solvent. With a higher cyclic capacity, less amount of solvent is required for the same removal. Hence, the cyclic capacity is an important parameter in determining the sensible heat requirement, pump work, size and cost of the absorbent-absorbent heat exchanger or cross exchanger. The CO_2 capacity is expressed as the product of the delta loading or CO_2 carrying effectiveness and the concentration of the alkalinity in the solvent.

$$\Delta C_{solve} = (\alpha_{rich} - \alpha_{lean})C_{K_2CO_3} \qquad (3.13)$$

33

Where $C_{K_2CO_3}$ is the concentration of K$_2$CO$_3$ in the solvent. Delta loading is determined by the solvent CO$_2$ VLE curve at 40°C. At a given mass concentration, the molar concentration of the absorbent is inversely proportional to its molecular weight so solvents with smaller molecular weights are preferred than that with bigger molecules, all else being equal.

3.2.1.6. Performance Parameters

The mass transfer driving force in the absorber is an important variable in the design of the process. The P^*_{CO2} in the solvent must be smaller than the P_{CO2} in the gas in the entire column to provide a positive driving force for the mass transfer. An absorber design that allows large mass transfer driving force to require less area and cost, but it can increase regeneration energy cost by producing irreversibility in the process. The overall mass transfer is given by –

$$N = K_G a \left(P_{CO_2} - P^*_{CO_2} \right) \qquad (3.14)$$

Where N is the molar flux of CO$_2$, K$_G$ is the overall mass transfer coefficient, a is the effective area and $P_{CO_2} - P^*_{CO_2}$ is the driving force. Typically, a log mean driving force, reflecting the driving force at the top and bottom of the column is used to estimate the flux if K$_G$ and a are known.

3.2.2. Regenerator/ Stripper

The solvent with rich CO$_2$ loading is sent to the stripper at a higher temperature (typically 80–150°C) where the CO$_2$ molecules are released from the

34

K_2CO_3 solution. After release of the CO_2 from the solvent, the CO_2 is sent to the condenser while the solvent with lean CO_2 loading circulates back to the absorber to absorb more CO_2 from the exhaust gas.

3.2.2.1. Stripper Temperature

A higher stripper operating temperature decreases the energy requirement for the process but can increase the rate of solvent loss due to degradation. Hence, the stripper temperature selection involves a trade-off between solvent loss and energy demands. Using an assumption for the acceptable rate of degradation of the solvent, the maximum stripper temperature (T_{max}) can be calculated from the first order degradation rate and the activation energy of the Arrhenius equation. Being an inert salt, K_2CO_3 is not prone to degradation. Therefore, the stripper temperature is only limited to exhaust enthalpy available at a given temperature.

3.2.2.2. Stripper Pressure

The stripper pressure will be fixed for a given temperature and loading. Higher stripper pressures reduce the amount of water vaporized per gmol of CO_2, as well as the compressor work. However, at a given stripper temperature, higher stripper pressures correspond to higher lean loadings, resulting in reduced solvent capacity and greater liquid circulation rates. For two solvents with the same capacity, higher stripper pressure is more desirable as it corresponds to lower compressor and stripping heat and hence lowers overall work. The stripper pressure is the sum of the partial pressure of CO_2, partial pressure of water and

the partial pressure of solvent at the stripper temperature. The partial pressure of CO_2 is assumed to be in equilibrium with the lean loading of the solvent at T_{max}.

3.2.2.3. Modelling the stripper

The VLE behavior of the system is estimated in Aspen Plus® Flash2™ model using an Electrolyte Non-Random Two-Liquid (ELECNRTL) method. The stripper pressure as well as the partial pressure of CO_2 and water in the solvent is obtained by using a flash calculation. The flash drum separates the incoming stream into vapor and liquid stream. The input parameters of the flash drum include a solvent stream and a CO_2 stream as shown in Figure 3.3. The solvent stream comprises of a solution of 40 wt% K_2CO_3 and water. The CO_2 stream comprises of CO_2 loadings that were varied from 0 – 1.0. The temperature of both the solvent stream and CO_2 stream were varied from 80°C – 200°C.
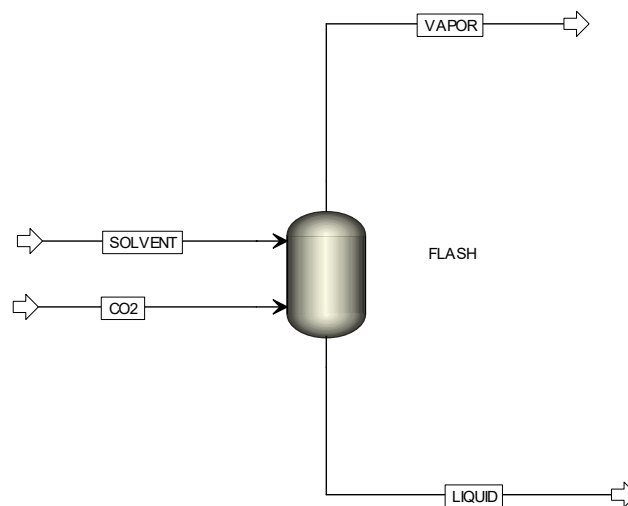
Figure 3.3. Simplified Aspen model flowsheet for Flash

36

The stripper or flash is represented with the help of a 2D Lookup table with XYZMap™ template in GT-Suite® labelled as Lookup flash. The X data represents the temperature of the solvent stream entering the stripper and is varied from 80-200°C while the Y data represents the CO_2 loading in the solvent stream entering the stripper and is varied from 0-1. The CO_2 loading range from 0-1 is converted to CO_2 mole fraction in the solvent stream before plotting it in the map. The X and Y data are the input parameters in the Lookup table. The Z data represents the total pressure generated at the stripper and is obtained from the flash calculation in Aspen Plus®. The flash generates two output streams: a vapor stream comprising of CO_2 and H_2O that goes to the condenser and a liquid stream comprising of K_2CO_3, H_2O and CO_2 that goes to the cross exchanger. An actuator is used to provide the output pressure of Lookup flash to the cross exchanger.

3.2.2.4. Regeneration Energy

The total energy generated at the stripper is the sum of the desorption energy, the sensible heat and the evaporation heat and is expressed as –

$$Q_{reg} = Q_{desorption} + Q_{sensible} + Q_{vaporization} \qquad (3.15)$$

$Q_{desorption}$ is the enthalpy change associated with CO_2 going from the gas phase to the liquid phase or vice-versa. This enthalpy change is negative (exothermic) for CO_2 absorption and positive for desorption and can be expressed as –

$$Q_{desorption} = -m_{CO_2} \Delta H_{absorption} \qquad (3.16)$$

37

The heat of absorption $\Delta H_{absorption}$ can be estimated directly from Aspen Plus® or from the temperature dependence of the partial pressure of CO_2 in equilibrium. The vapor pressure data generated by the flash calculation can be used in the Clausius-Clapeyron equation given by equations 3.17 – 3.18.

$$\Delta H_{absorption} = R \left(\frac{\partial \ln P_{CO_2}^*}{\partial \frac{1}{T}} \right)_{P, \ x} \qquad (3.17)$$

$$ln \left(\frac{P_{CO2,lean|Tmax}^*}{P_{CO2,lean|40°C}^*} \right) = \frac{-\Delta H_{abs}}{R} \left(\frac{1}{T_{max}} - \frac{1}{T_a} \right) \qquad (3.18)$$

Where T_{max} is the maximum stripper temperature, R is the universal gas constant. The Clausius-Clapeyron equation assumes that molar volume of liquid is negligible relative to the molar volume of vapor and the heat of addition is independent of the temperature (Smith et. al., 1996).

$Q_{sensible}$ is the amount of energy required to heat the solvent to the stripper temperature.

$$Q_{sensible} = \frac{flow \ rate \ of \ solvent}{flow \ rate \ of \ CO_2} \qquad (3.19)$$

Which can also be expressed as –

$$Q_{sensible} = \dot{m}_{solvent,R} \ C_{p_{solvent}} \Delta T \qquad (3.20)$$

Where $Cp_{solvent}$ is the specific heat capacity of the solvent at the rich loading (kJ/kgK). The approach temperature ΔT is the temperature difference of the solvent from the cross exchanger to the stripper.

$Q_{vaporization}$ is the amount of heat generated due to vaporization of water from the solvent. When the temperature of the solvent is increased on its way to the stripper, some amount of water is vaporized from the solvent.

$$Q_{vaporization} = m_{CO_2}^{\cdot} \frac{P_{H_2O} \, \Delta H_{vaporization,H_2O}}{P_{CO_2}} \qquad (3.21)$$

Where $\Delta H_{vaporization,H2O}$ is the enthalpy of vaporization of water. P_{CO2} and P_{H2O} are the partial pressures of CO_2 and water in the solvent.

3.2.3. Heat exchangers

There CO_2 capture system comprises of two heat exchangers that increases the temperature of the solvent before it is sent to the stripper.

3.2.3.1. Exhaust-Absorbent Heat Exchanger

The exhaust-absorbent heat exchanger reduces the temperature of the exhaust gas coming from the SCR. The heat is rejected to the solvent stream with rich loading leaving the cross exchanger thereby increasing the temperature of the solvent stream to the desired operating temperature of the stripper. The amount of heat rejected also provides the sensible heat, the heat for desorption of CO_2 and

39

the heat of vaporization of water. The heat rejected by the exhaust gas is given by

–

$$Q_{exh-a\ ,HR} = Q_3 = \dot{m}_{exhaust} C_{p_{exhaust}} (T_1 - T_2) \qquad (3.22)$$

$Q_{exh-abs,HR}$ is the amount of heat energy rejected by the exhaust stream. T_1 and T_2 are the temperature of the exhaust gas entering and leaving the exhaust-absorbent heat exchanger. The exhaust gas flow rate, $\dot{m}_{exhaust}$ and temperature, T_1 are obtained from the SET data. The specific heat capacity of exhaust gas is estimated to be 1.014 kJ/kgK. The temperature of the exhaust stream should be maintained at 40-60°C for the CO_2 absorption process, as the carbon molecules break away from the solvent molecular bond at higher temperature. Hence, the outlet temperature of exhaust gas, T_2 is assumed to be 40°C. The effectiveness of the heat exchanger is assumed as 0.85. Hence, the amount of heat rejected is estimated by putting these values in the equation 3.22.

As the heat exchange process occurs with the solvent stream with rich loading leaving the cross exchanger, the amount of heat energy gained by the solvent stream is given by the following equation.

$$Q_{exh-a\ ,HA} = \dot{m}_{solvent,R} C_{p_{solvent,R}} (T_4 - T_3) = \dot{m}_{solvent,R} C_{p_{solvent,R}} \Delta T_{3-4} \qquad (3.23)$$

Where $Q_{exh-abs,HA}$ is the sensible heat, or the amount of heat energy added to the solvent stream. $\dot{m}_{solvent,R}$ is flow rate of the solvent and is calculated from the absorber mass balance equation while $Cp_{solvent,R}$ is the specific heat capacity of

40

the solvent with rich loading, which is obtained from the ELECNRTL method in Aspen Plus®. T_4 and T_3 are the temperatures of the solvent stream with rich loading entering and leaving the exhaust-absorbent heat exchanger and are assumed to have a temperature difference, $\Delta T_{3\text{-}4}$ of 10°C.

The remaining heat energy is used to provide the heat for desorption of CO_2 and the heat of vaporization of water and is given by –

$$Q_{exh-abs,HR} - Q_{exh-a\ ,HA} \qquad (3.24)$$

The exhaust-absorbent heat exchanger is modelled in GT-Suite® with an HXMaster™ and HXSlave™ template as shown in Figure 3.4. The rich CO_2 solvent stream passes through the HXMaster™ unit (Exh-Abs_HX-1) while the exhaust stream passes through the HXSlave™ unit (Exh-Abs_HX).

41
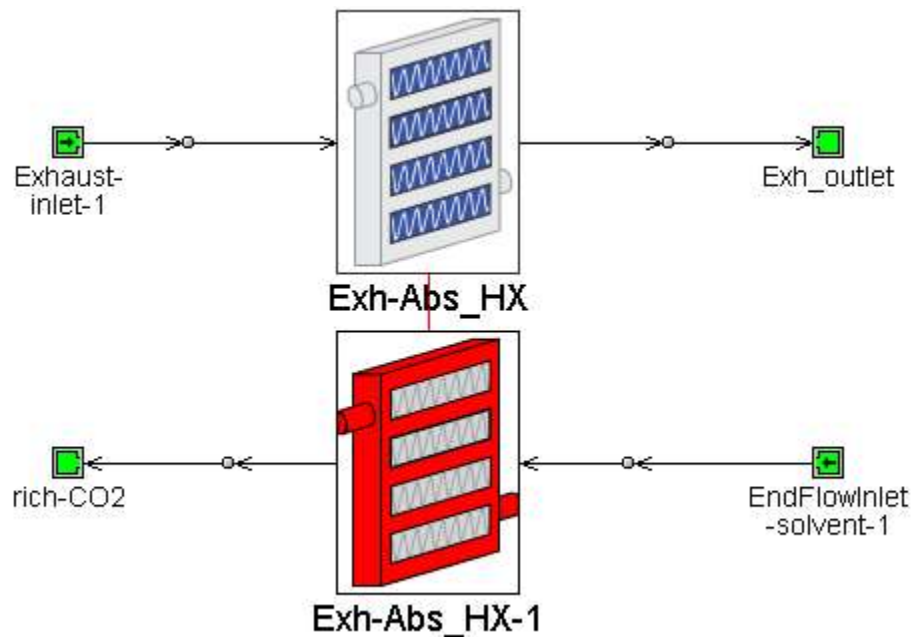
Figure 3.4. GT-Suite model of Exhaust-Absorbent heat exchanger

Table 3.2 and 3.3 shows the input parameters for HXSlave™ and HXMaster™ respectively. The input properties of the solvent such as flow rate and composition are determined from the absorber mass balance equation.

Table 3.2. Input parameters of exhaust gas for HXSlave™ (Exh-Abs_HX)

Exhaust gas temperature (°C)	354.4
Pressure (bar)	1
Composition (%)	CO_2=8.33, H_2O=3.1, N_2=62, O_2=26.57
Exhaust flow rate (kg/s)	0.2254

Table 3.3. Input parameters of solvent for HXMaster™ (Exh-Abs_HX -1)

Solvent inlet temperature (°C)	110
Solvent outlet temperature (°C)	120

42

Solvent Composition (%) and Solvent flow rate (kg/s)	Obtained from absorber mass balance results

The heat exchanger design specifications are obtained from that of a TubeFin Air-Air Charge Air Cooler (CAC) for a sample truck with scaling object defined. Table 3.4 shows the design specifications of the heat exchanger.

Table 3.4. Heat exchanger design specifications

Heat exchanger height (mm)	672
Heat exchanger width (mm)	895
Heat exchanger depth (mm)	63
Inlet connection diameter (mm)	55
Outlet connection diameter (mm)	55
Tube and fin material	Aluminium
Mass of fin and tube material (kg)	6

43

Tube wall thickness (mm)	1
Number of channels in a tube (mm)	35
Number of passes	1
Number of tubes per pass	50
Tube flow orientation	Horizontal

3.2.3.2. Absorbent-Absorbent Heat Exchanger

The absorbent-absorbent heat exchanger or cross exchanger increases the temperature of the solvent stream with rich loading coming from the absorber before it goes to the stripper. The heat exchange process occurs between the cold rich solvent stream leaving the absorber and the hot lean solvent stream coming out of the stripper. The amount of heat rejected is given by the following equation.

$$Q_{cross,HR} = Q_4 = \dot{m}_{solvent,R} C_{p_{solvent,R}} (T_3 - T_2) = \dot{m}_{solvent,R} C_{p_{solvent,R}} \Delta T_{2-3} \qquad (3.25)$$

Where $Q_{cross,HR}$ is the heat rejected by the solvent stream with rich loading, $\dot{m}_{solvent,R}$ is flow rate of the solvent with rich loading and is calculated from the absorber mass balance equation and $Cp_{solvent,R}$ is the specific heat capacity of the solvent

44

with rich loading that is obtained from the ELECNRTL method in Aspen Plus®. T_2 and T_3 are the temperatures of the solvent stream with rich loading entering and leaving the cross exchanger respectively. T_2 is maintained at 40°C as assumed in the absorber. As we have considered an approach temperature of 10°C for the sensible heat in the regenerator, T_3 is assumed to be 110°C. The heat exchanger effectiveness is assumed as 0.85.

The heat transfer occurs with the hot liquid stream or lean solvent stream leaving the stripper or flash. Hence, the amount of heat energy gained by the solvent stream with lean loading is given by the following equation.

$$Q_{cross,HA} = \dot{m}_{solvent,L} C_{p_{solvent,L}} (T_4 - T_5) = \dot{m}_{solvent,L} C_{p_{solvent,L}} \Delta T_{5-4} \qquad (3.26)$$

Where $Q_{cross,HA}$ is the amount of heat energy added to the solvent stream with lean loading. $\dot{m}_{solvent,L}$ is flow rate of the solvent with lean loading and is calculated from the absorber mass balance equation and $C_{p_{solvent,L}}$ is the specific heat capacity of the solvent with lean loading that is obtained from the ELECNRTL method in Aspen Plus®. T_4 is the temperature of the solvent stream leaving the stripper and is at the same temperature as the stripper while T_5 is the temperatures of the solvent stream with lean loading leaving the cross exchanger and entering the trim cooler.

The cross exchanger is modelled using an HXMaster™ and HXSlave™ template in GT-Suite® as shown in Figure 3.5, where the solvent with rich CO_2 loading passes through the HXMaster™ (Cross_EX-1) and the solvent with lean CO_2 loading passes through the HXSlave™ unit (Cross_EX).
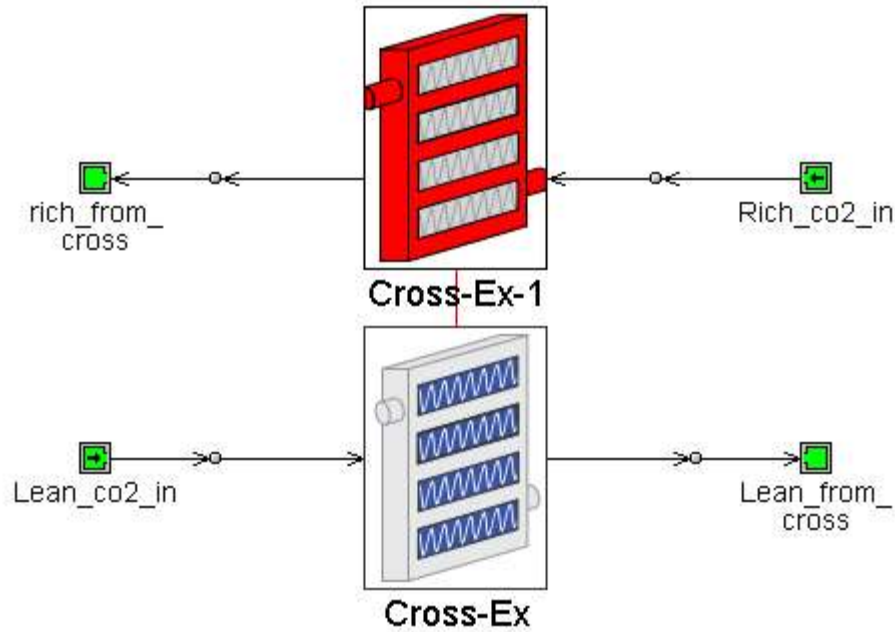
Figure 3.5. GT-Suite model of Cross exchanger

The heat exchanger specifications are kept same as that of exhaust-absorbent heat exchanger shown in Table 3.4. Table 3.5 and Table 3.6 lists the input parameters for the two units. The solvent flow rates and composition for both streams are calculated from the absorber mass balance equation.

Table 3.5. Input parameters of rich solvent for HXMaster™ (CrossEx-1)

Rich CO_2 solvent inlet temperature (°C)	40
Rich CO_2 solvent outlet temperature (°C)	110

46

Solvent Composition (%) and Solvent flow rate (kg/s)	Obtained from absorber mass balance results

Table 3.6. Input parameters of lean solvent for HXSlave™ (CrossEx)

Lean CO_2 solvent inlet temperature (°C)	120
Lean CO_2 solvent outlet temperature (°C)	50
Solvent Composition (%) and Solvent flow rate (kg/s)	Obtained from absorber mass balance results

3.2.4. Cooler

The CO_2 capture system comprises of a trim cooler that brings down the temperature of the solvent stream coming from the stripper to the temperature required for the CO_2 absorption process.

47

3.2.4.1. Trim Cooler

The trim cooler maintains the temperature required for the absorber after the solvent circulates back from the high temperature stripper. The amount of heat rejected by the trim cooler is given by –

$$Q_{trim} = Q_5 = \dot{m}_{solvent,L} C_{p_{solvent,L}}(T_5 - T_2) = \dot{m}_{solvent,L} C_{p_{solvent,L}} \Delta T_{2-5} \qquad (3.28)$$

Where $\dot{m}_{solvent,L}$ is flow rate of the solvent with lean CO_2 and is calculated from the absorber mass balance equation and $Cp_{solvent,L}$ is the specific heat capacity of the solvent with lean loading which is obtained from the ELECNRTL method in Aspen Plus®. T_5 and T_2 are the temperatures of the solvent stream with lean loading entering and leaving the trim cooler. T_2 is assumed as 40°C in the absorber due to the low temperature requirement of the CO_2 absorption process. The temperature difference of the trim cooler, ΔT_{2-5} is assumed as 10°C.

The trim cooler is modelled using an HXMaster™ and HXSlave™ template in GT-Suite® as shown in Figure 3.7. Water is passed through the HXMaster™ unit (Trim-cooler-1) while the solvent stream with lean CO_2 exiting the cross exchanger passes through the HXSlave™ unit (Trim-cooler).

48

Figure 3.6. GT-Suite model of Trim cooler

The heat exchanger specifications are kept same as that of exhaust-absorbent heat exchanger as shown in Table 3.4. The input parameters of the two units are listed in Table 3.9 and 3.10.

Table 3.7. Input parameters of lean CO_2 solvent for HXSlave™ (TrimCooler)

Lean CO_2 solvent inlet temperature (°C)	50
Lean CO_2 solvent outlet temperature (°C)	40

49

Solvent Composition (%) and Solvent flow rate (kg/s)	Obtained from absorber mass balance results

3.2.5. Condenser

The condenser condenses the vapor stream leaving the stripper or flash before it enters the compressor. The vapor stream comprises of CO_2 and H_2O. After leaving the condenser, the water from the stream is drained and is recirculated back into the stripper. The condensed CO_2 stream then goes to the compressor where it is compressed for storage.

The cooling duty for steam or the amount of heat rejected due to vaporization of water is given by the following equation.

$$Q_{H_2O} = m_{H_2O} \Delta H_{vaporization, H_2O} \qquad (3.29)$$

Where $\dot{m}_{H2O}$ is the mass flow rate of water in the vapor stream and $\Delta H_{vaporization,H2O}$ is the latent heat of vaporization of water. The latent heat of vaporization of water is 2257 kJ/kgK.

The amount of heat rejected in condensing CO_2 is given by equation 3.30.

$$Q_{CO_2} = m_{CO_2} C_{p_{CO_2}} (T_4 - T_6) \qquad (3.30)$$

50

Where $\dot{m}_{CO2}$ is the mass flow rate of CO_2 in the vapor stream and Cp_{CO2} is the specific heat capacity of CO_2. T_4 is the temperature of the vapor stream leaving the stripper while T_6 is the outlet temperature of the stream leaving the condenser, which we have assumed as 40°C.

The flash calculation in Aspen Plus® provides the total pressure at the stripper, P_{total} and the mole fraction of CO_2, y_{CO2} and mole fraction of H_2O, y_{H2O} in the vapor stream for a temperature of 80-200°C and a CO_2 loading of 0-1. Using the Dalton's law of partial pressure, we can calculate the mole fraction of CO_2 and H_2O using the following equations.

$$P_{CO_2} = y_{CO_2} P_{total} \qquad (3.31)$$

$$P_{H_2O} = y_{H_2O} P_{total} \qquad (3.32)$$

Using equations 3.31 and 3.32, we can obtain the partial pressure of CO_2 and H_2O for a temperature range of 80-200°C and a CO_2 loading of 0-1. The data obtained for both partial pressure of CO_2 and H_2O are plotted in 2D Lookup tables using XYZMap™ template in GT-Suite®. The lookup table for partial pressure of CO_2 is labelled as Lookup_flash-CO_2 and the lookup table for partial pressure of H_2O is labelled as Lookup_flash-H_2O. The input parameters for both tables comprises of the flash output temperature of 80-200°C as X data and CO_2 loading of 0-1 converted to mole fractions of CO_2 in the solvent stream as Y data. The Z data gives the partial pressure of CO_2 and the partial pressure of H_2O as the output. The output pressure from both the lookup tables is sensed by an actuator and is

51

provided as an input to the condenser. Using the temperature and the partial pressure of CO_2 and H_2O as inputs, we can calculate the cooling duty for steam and CO_2 in the condenser.

The condenser is modelled in GT-Suite® with an HXMaster™ and HXSlave™ template as shown in Figure 3.8. Water is passed through the HXMaster™ unit (Condenser-1). The CO_2 vapor stream from lookup table for partial pressure of CO_2 (Lookup_flash-CO_2) and the H_2O vapor stream from lookup table for partial pressure of H_2O (Lookup_flash-H_2O) passes through the HXSlave™ unit (Condenser-2).
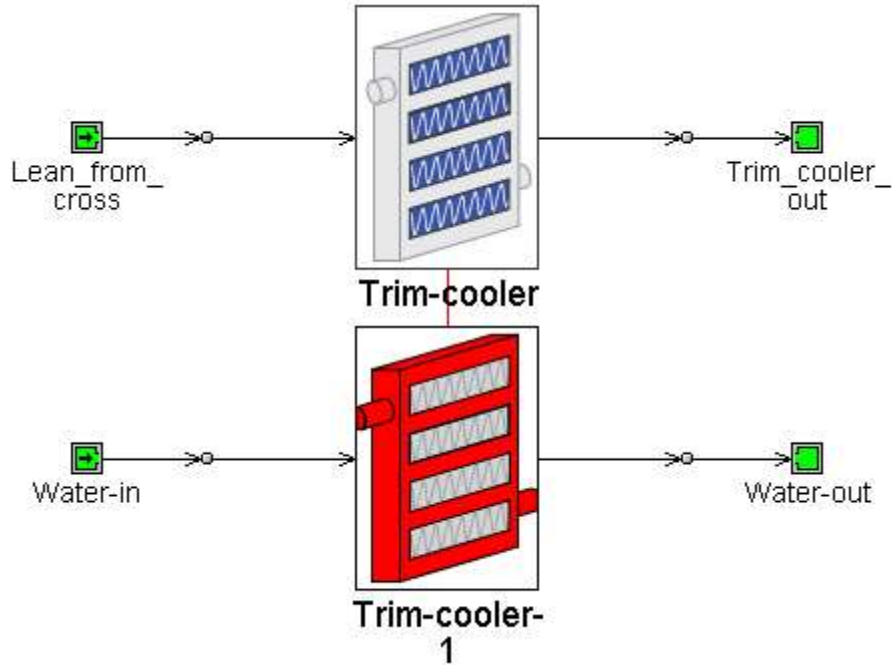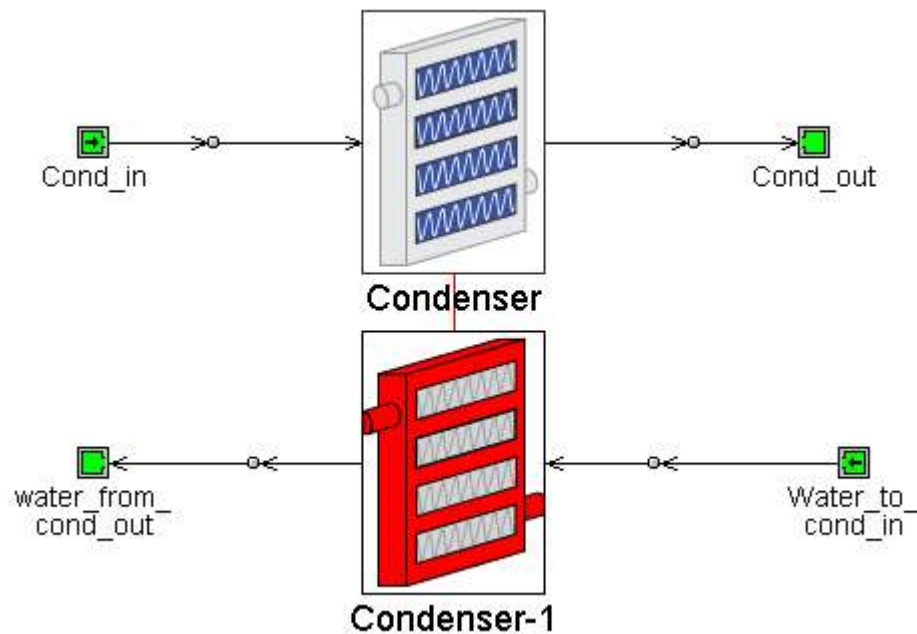

Figure 3.7. GT-Suite model of Condenser

The condenser specifications are kept same as that of exhaust-absorbent heat exchanger as shown in Table 3.4. The input parameters for HXMaster™ and HXSlave™ for the condenser at B50 operating point are listed below.

Table 3.8. Input parameters of vapor stream from flash for HXSlave™
(Condenser)

Vapor stream inlet temperature (°C)	120
Outlet temperature (°C)	40
Composition	H_2O, CO_2
CO_2 flow rate (kg/s)	0.01
H_2O flow rate (kg/s)	0.068

3.2.6. Compressor

The compressor compresses the incoming stream of CO_2 from the stripper through the condenser for storing it in the tank. The CO_2 stream remains in the vapor form when it enters the compressor. Assuming isentropic compression, the compressor work is calculated using an empirical correlation developed by Van Wagner (2011), given by –

53

$$W_{comp} = \frac{4.572 * \ln\left(\frac{P_{out}}{P_{in}}\right) - 4.096}{\eta_{comp}} \qquad (3.33)$$

Where P_{out} is the pressure at which the CO_2 would be compressed before storage and P_{in} is the pressure of the vapor stream coming out of the stripper. η_{comp} is the efficiency of the compressor.

A PumpFlow™ template is used to model the compressor in GT-Suite® that determines the work required to compress the CO_2 stream exiting the condenser. The input parameters for the compressor are shown in Table 3.13.

Table 3.9. Input parameters of the compressor (PumpFlow™)

Mass flow rate of CO_2 stream (kg/s)	0.01
Inlet Pressure, P_{in} (bar)	Total pressure generated in stripper at 120°C
Outlet Pressure, P_{out} (bar)	100
Isentropic efficiency (%)	85

3.3. Model Development in GT-Power®

The heat exchangers, coolers and condenser, modelled individually in GT-Suite® are then integrated along with the lookup tables for total pressure and the partial pressure of CO_2 and H_2O to form the CO_2 capture system as shown in Figure 3.9.
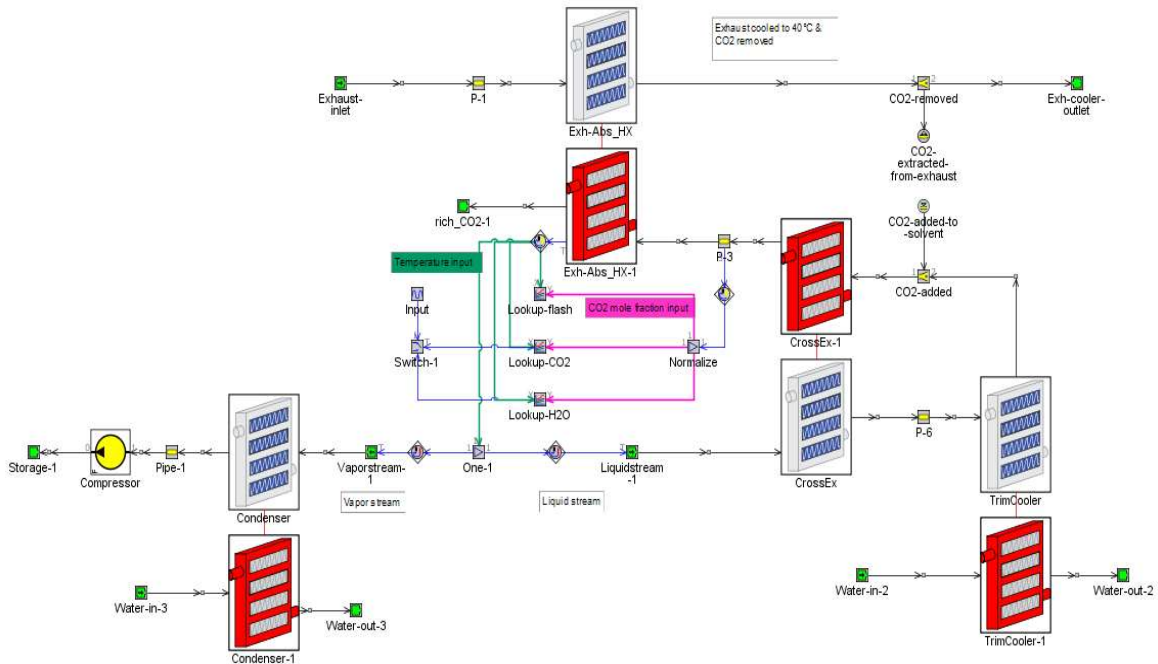
Figure 3.8. GT-Power model of the CO_2 Capture System

The exhaust gas is sent through the exhaust-absorbent heat exchanger where its temperature is reduced. A CO_2 ejector removes the specified amount of CO_2 from the exhaust before it is sent to the exhaust outlet. The amount of CO_2 removed is then added to the solvent stream by a CO_2 Injector before it is sent to the cross exchanger. The cross exchanger and the exhaust-absorbent heat exchanger

55

increases the solvent temperature to the desired temperature of the stripper. The green lines from the exhaust-absorbent heat exchanger senses the temperature input while the pink lines from the cross exchanger senses the CO_2 loading which is converted to CO_2 mole fraction. Three lookup tables are generated for total pressure (Lookup-flash), partial pressure of CO_2 (Lookup-CO_2) and partial pressure of H_2O (Lookup-H_2O) at the stripper as a function of temperature and CO_2 loading or CO_2 mole fraction. The vapor stream from the stripper is sent to the condenser while the liquid stream is sent to the cross exchanger and the trim cooler where more CO_2 is injected from exhaust gas. The output from the Lookup-CO_2 and the Lookup-H_2O is actuated to the vapor stream entering the condenser. A switch is provided to send the pressure output for either CO_2 stream or H_2O stream at one time, to the condenser. The One-1 senses the temperature input to the condenser and the cross-exchanger. The compressor is connected to the condenser to compress the CO_2 to the desired pressure.

Chapter 4

Results and Discussion

This chapter discusses the results obtained from the VLE behavior of the system and the heat rate for different operating points along with the thermodynamic and chemical calculations in the CO_2 capture system and its subcomponents.

4.1. Results from Aspen Plus® Flash

The flash drum is maintained at a temperature of 120°C and comprises of two input streams: one stream had 40 wt.% K_2CO_3 and water while the other stream had CO_2 loading. Using sensitivity analysis, the temperature of the two input streams are varied from 80°C – 200°C. The CO_2 loading was varied from 0 – 1.0 which was converted to mole fraction of CO_2 in the solvent stream. The flash drum generates two output streams: a vapor stream and a liquid stream. The vapor stream comprises of CO_2 and H_2O and is sent to the condenser while the liquid stream circulates back as the solvent to absorb more CO_2 from the absorber. The total pressure generated in the stripper is represented as a function of the

temperature of the solvent stream exiting the exhaust-absorbent heat exchanger and the CO_2 loading in the same. Figure 4.1 shows the plot of total pressure generated in the stripper for a temperature range of 80°C – 200°C and a CO_2 loading of 0 – 1.0 in the solvent stream.
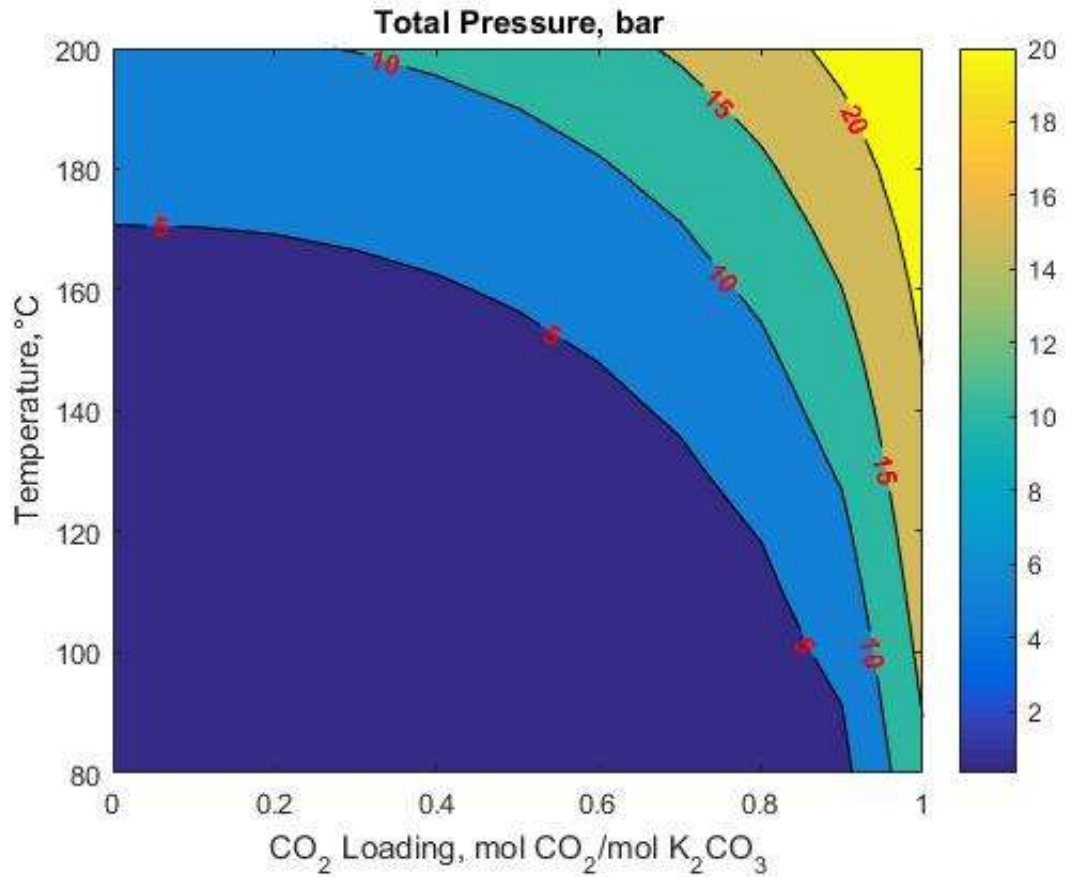
Figure 4.1. Total pressure at the stripper at a temperature of 80 – 200°C and CO_2 loading from 0 – 1.0.

58

4.1.1. Calculation of partial pressure of CO_2 and H_2O

The total pressure generated at the stripper can be expressed as the sum of the partial pressures of CO_2, H_2O and K_2CO_3. Using sensitivity analysis for the flash drum, the composition of the individual components were calculated for both vapor and liquid stream. Using the Dalton's law of partial pressure, the partial pressure of CO_2 and H_2O in the stripper were calculated as a function of the temperature and CO_2 loading of the solvent inlet stream and are shown in Figure 4.2 and 4.3 respectively. The partial pressure of CO_2 and H_2O obtained from the results are then used to determine the heat of vaporization of water at the stripper to calculate the total regeneration energy required for the CO_2 desorption process.
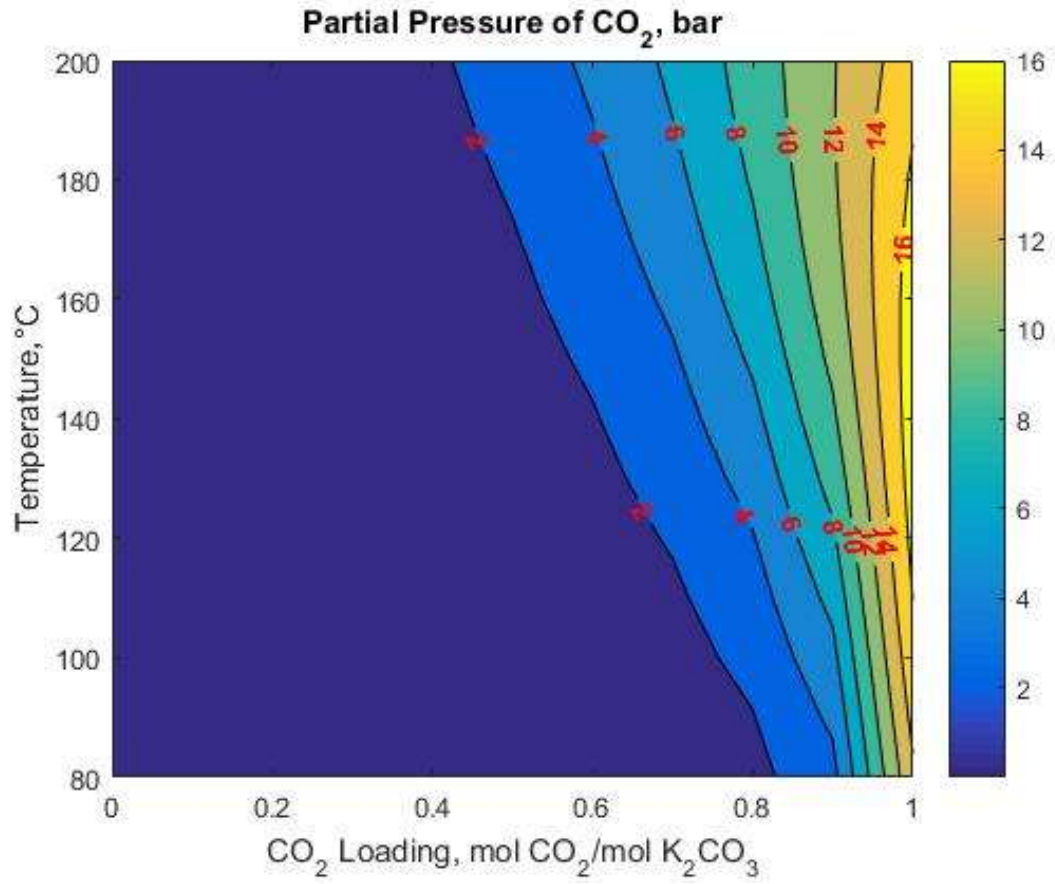
Figure 4.2. Partial pressure of CO_2 at a temperature of 80 – 200°C and CO_2
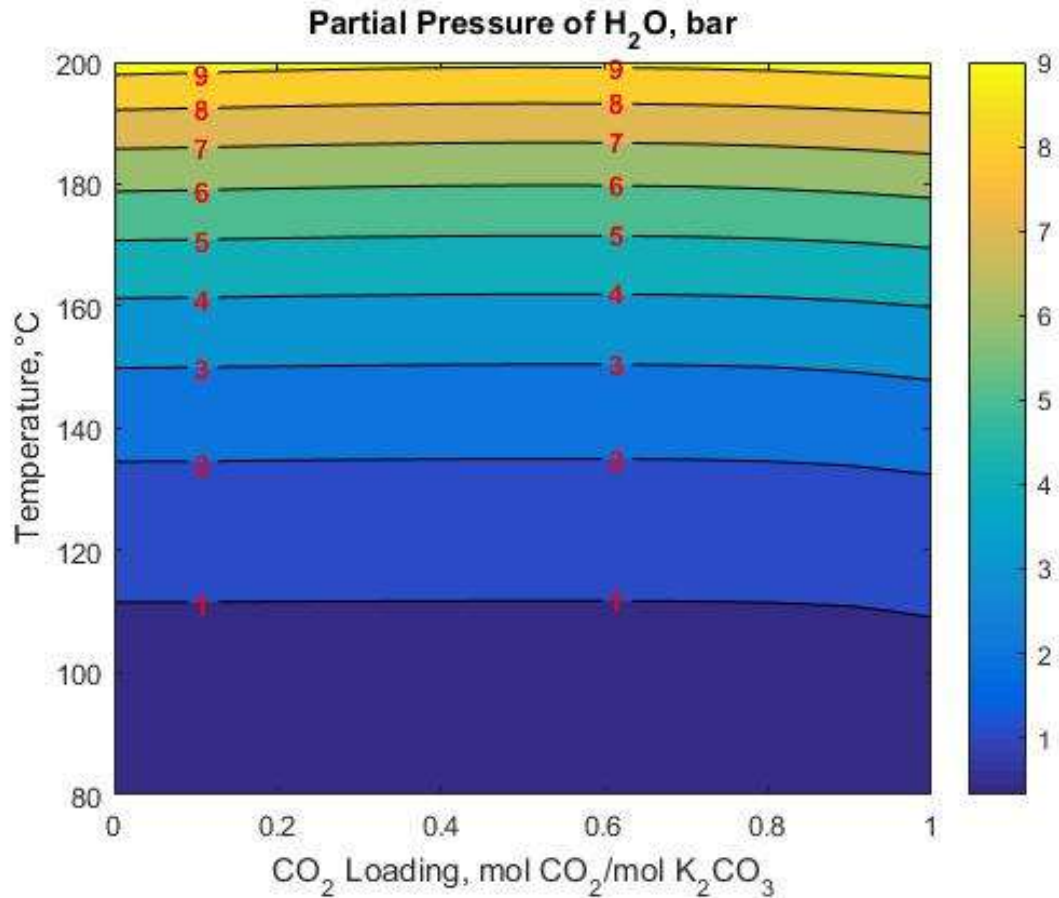
loading from 0 – 1.0.

Figure 4.3. Partial pressure of H_2O at a temperature of $80 - 200°C$ and CO_2 loading from $0 - 1.0$.

4.1.2. Vapor Liquid Equilibrium in 40 wt.% K_2CO_3 system

In 1959, Tosh et. al conducted equilibrium studies in a rocking autoclave unit and determined the equilibrium behavior of K_2CO_3-$KHCO_3$-CO_2-H_2O system with 40 wt.% K_2CO_3 for a temperature range of $343 - 413$ K. The VLE results are obtained for 40 wt.% K_2CO_3 by using flash calculations in Aspen Plus® for a temperature range of $80 - 200°C$. Figure 4.4 shows a comparison of the

61

experimental results from Tosh and Aspen results from flash for a temperature of 110°C and 130°C. There is a slight deviation of the Aspen values from those of the experimental values. The deviation is significant especially in case of higher temperature and loadings. The solution would remain close to a temperature around 110°C which is the boiling point of the solvent with 40 wt.% K_2CO_3.
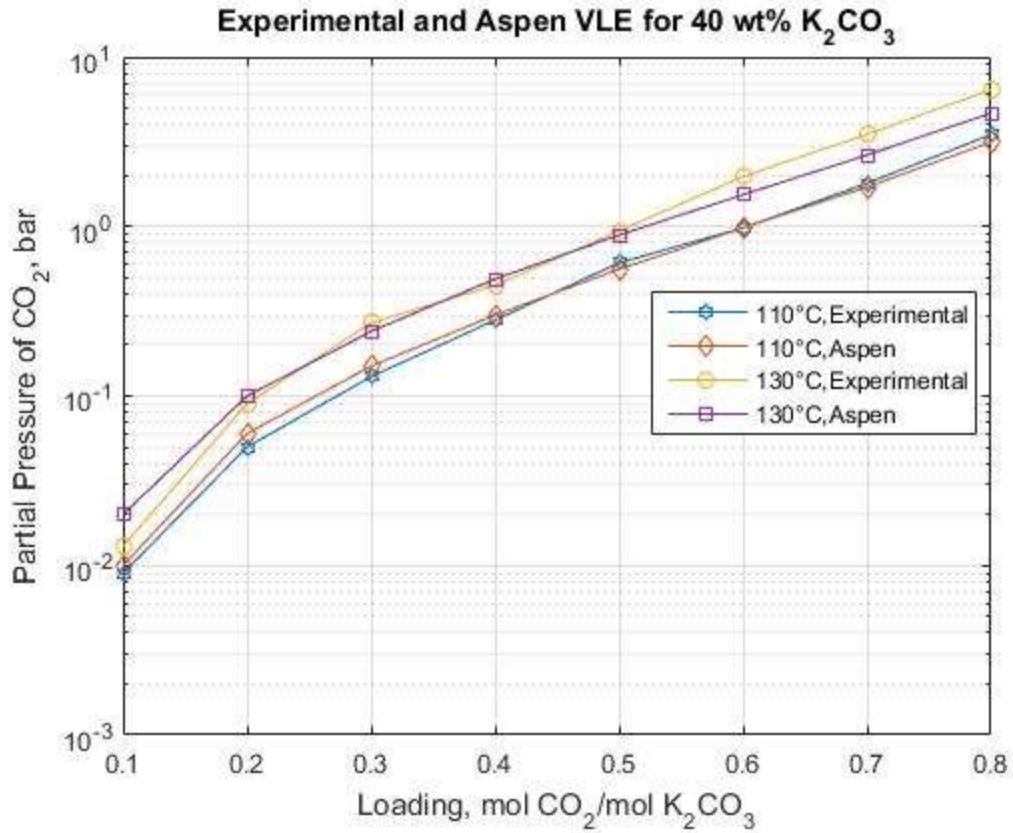
Figure 4.4. Comparison of the experimental behavior from Tosh et. al (1959) and Aspen VLE at a temperature of 110°C and 130°C

4.2. Calculation of Absorber parameters

For the operating point B50, the gas flow rate leaving the absorber, G_2 and the CO_2 composition of the exhaust stream leaving the absorber, y_2 can be calculated using equations 3.6 – 3.10. From Table 3.1 and using equation 3.7, the molar flow rate of CO_2 entering the absorber can be estimated.

$$n_1 = y_1 G_1$$

$$n_1 = 0.0833 \left(\frac{mol}{mol}\right) * \frac{811.44 \left(\frac{kg}{hr}\right)}{29 \left(\frac{g}{mol}\right)}$$

$$n_1 = 0.647 \frac{mol}{s}$$

With a CO_2 capture rate of 60%, the molar flow rate of CO_2 in the exhaust stream leaving the absorber can be calculated using the following equation.

$$CO_2 \ Capture \ rate(\%) = \frac{n_1 - n_2}{n_1} 100(\%)$$

$$60 = \frac{n_1 - n_2}{n_1} 100(\%)$$

$$60 = \frac{0.647 - n_2}{0.647} 100(\%)$$

$$n_2 = 0.258 \frac{mol}{s}$$

63

With the newly obtained value of n_2, the exhaust flow rate leaving the absorber, G_2 can be determined by using the following equation.

$$G_2 = G_1 - n_1 + n_2$$

$$G_2 = 7.77 \frac{mol}{s} - 0.647 \frac{mol}{s} + 0.258 \frac{mol}{s}$$

$$G_2 = 7.38 \frac{mol}{s}$$

$$G_2 = 7.38 \frac{mol}{s} * 29 \frac{g}{mol}$$

$$G_2 = 770.82 \frac{kg}{hr}$$

Hence, the CO_2 composition in the exhaust stream leaving the absorber, y_2 can be determined by the following equation.

$$y_2 = \frac{n_2}{G_2}$$

$$y_2 = \frac{0.258 \frac{mol}{s}}{7.38 \frac{mol}{s}}$$

$$y_2 = 0.035 \frac{mol}{mol}$$

4.2.1. Loading calculation and optimization

The exhaust gas parameters can be obtained from Table 3.1. For the operating point B50, the partial pressure of CO_2 of the exhaust stream entering and leaving the absorber can be calculated from total pressure and CO_2 composition using Dalton's law of partial pressure. For the exhaust stream entering the absorber,

$$P_{CO_2,\ 1g} = Py_1$$

$$P_{CO_2,\ 1g} = 1\ bar * 0.0833\ \frac{mol}{mol}$$

$$P_{CO_2,\ 1g} = 0.0833\ bar$$

For the exhaust stream leaving the absorber, the partial pressure of CO_2 in the gas is given by –

$$P_{CO_2,\ 2g} = Py_2$$

$$P_{CO_2,\ 2g} = 1\ bar * 0.035\ \frac{mol}{mol}$$

$$P_{CO_2,\ 2g} = 0.035\ bar$$

In the above calculations, $P_{CO2,\ 1}$ and $P_{CO2,\ 2}$ are the partial pressure of CO_2 in the gas. The difference between the partial pressure of CO_2 in gas and the equilibrium partial pressure of CO_2 in liquid represents the driving force for the mass transfer

65

of absorber. Assuming the driving force for mass transfer as a factor of 2, the partial pressure of CO_2 in the liquid leaving and entering the absorber can be obtained by the following equations.

$$P_{CO_2,\ 1l} = \frac{P_{CO_2,\ 1g}}{2} = 0.0416\ bar$$

$$P_{CO_2,\ 2l} = \frac{P_{CO_2,\ 2g}}{2} = 0.0175\ bar$$

Figure 4.5 shows the plot of partial pressure of CO_2 with respect to the CO_2 loading at 40°C as obtained from the Aspen results. The partial pressure of CO_2 obtained from the above equations can be compared to the plot to obtain the corresponding CO_2 loading in the solvent entering and leaving the absorber. From Figure 4.5, at $P_{CO2,\ 1L}$ = 0.0416 bar, the corresponding CO_2 loading or rich loading is 0.44 mol CO_2/mol K_2CO_3 and at $P_{CO2,\ 2L}$ = 0.0175 bar, the CO_2 loading or lean loading is 0.31 mol CO_2/mol K_2CO_3.
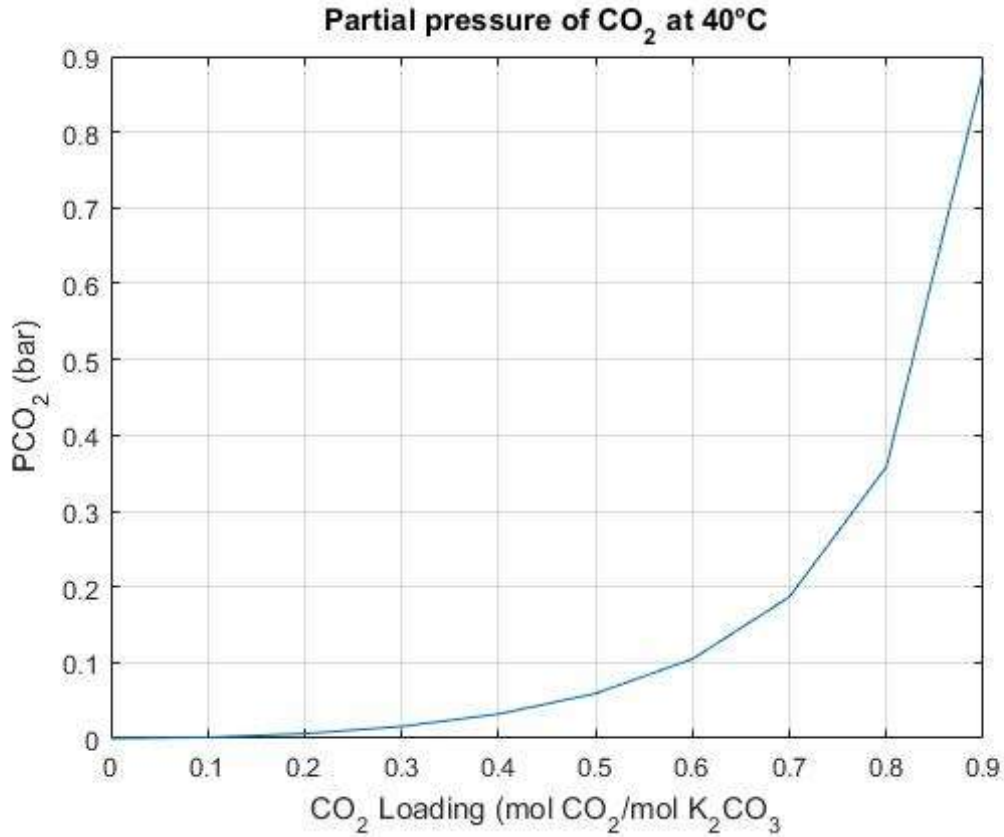
Figure 4.5. Partial pressure of CO_2 with respect to CO_2 loading at 40°C for a 40

wt.% K_2CO_3 system solvent as obtained from Aspen results

4.2.2. Calculation of solvent flow rate

Using equations 3.2 – 3.5, we can calculate the number of moles of K_2CO_3,

CO_2 and H_2O in the solvent stream entering the absorber.

$$n_{K_2CO_3} = \frac{40 \ x \ 100gm}{138.205g/mol} = 28.94 \ mol$$

$$n_{H_2O} = \frac{60 \ x \ 100gm}{18.01g/mol} = 333.14 \ mol$$

67

Moles of CO_2 in the absorber inlet stream,

$$n_{CO_{2,\ 2}} = 28.94\ mol * 0.31 = 8.97\ mol$$

Mole fraction of CO_2 in the solvent entering absorber,

$$x_{CO_{2,\ 2}} = \frac{8.97}{28.94 + 333.14 + 8.97} = 0.024\ \frac{mol}{mol}$$

Moles of CO_2 in absorber outlet stream,

$$n_{CO_{2,\ 1}} = 28.94\ mol * 0.44 = 12.73\ mol$$

Mole fraction of CO_2 in the solvent leaving absorber,

$$x_{CO_{2,\ 1}} = \frac{12.73}{28.94 + 333.14 + 12.73} = 0.035\ \frac{mol}{mol}$$

Hence, solvent flow rate entering absorber = L_2

Mol flow rate of CO_2 entering absorber,

$$m_2 = L_2 * x_{CO_{2,\ 2}} = L_2 * 0.024\ \frac{mol}{mol}$$

Mol flow rate of CO_2 leaving absorber,

$$m_1 = L_1 * x_{CO_{2,\ 1}} = L_1 * 0.035\ \frac{mol}{mol}$$

Solvent flow rate leaving absorber,

$$L_1 = L_2 - m_2 + m_1$$

68

$$L_1 = L_2 - (L_2 * 0.024) + (L_1 * 0.035)$$

$$L_1 = L_2 * \frac{1 - 0.024}{1 - 0.035} = L_2 * 1.01$$

From absorber mass balance equation or equation 3.1,

$$L_1 * 0.035 \frac{mol}{mol} + 7.6 \frac{mol}{s} * 0.034 \frac{mol}{mol} = L_2 * 0.024 \frac{mol}{mol} + 8 \frac{mol}{s} * 0.0833 \frac{mol}{mol}$$

$$(L_2 * 1.011) * 0.035 \frac{mol}{mol} + 7.6 \frac{kg}{hr} * 0.034 \frac{mol}{mol}$$

$$= L_2 * 0.024 \frac{mol}{mol} + 8 \frac{mol}{s} * 0.0833 \frac{mol}{mol}$$

$$L_2 = 3647.82 \frac{kg}{hr} = 1.12 \frac{kg}{s}$$

$$L_1 = 3720.68 \frac{kg}{hr} = 1.14 \frac{kg}{s}$$

$$\frac{L_1}{G_1} = 4.4 \ and \ \frac{L_2}{G_2} = 4.6$$

Using the same procedure, the CO_2 lean and rich loadings as well as the liquid flow rates entering and leaving the absorber can be evaluated for all the SET points as shown in Table 4.1.

69

Table 4.1. CO_2 loadings and solvent flow rates entering and leaving the absorber for SET points A25-C100

SET Points	Lean Loading (mol CO_2/ mol K_2CO_3)	Rich Loading (mol CO_2/ mol K_2CO_3)	Liquid flow rate entering absorber, L_2 (kg/s)	Liquid flow rate leaving absorber, L_1 (kg/s)
A25	0.30	0.42	0.53	0.54
A50	0.32	0.45	0.93	0.94
A75	0.34	0.47	1.32	1.34
A100	0.34	0.47	1.77	1.80
B25	0.30	0.42	0.64	0.65
B50	0.31	0.44	1.12	1.14
B75	0.32	0.45	1.60	1.63
B100	0.33	0.46	2.13	2.16
C25	0.29	0.41	0.72	0.73
C50	0.31	0.43	1.23	1.25

C75	0.32	0.44	1.73	1.75
C100	0.33	0.45	2.22	2.25

4.3. Calculation of regeneration energy

4.3.1. Heat of Absorption calculation

The heat of absorption of 40 wt.% K_2CO_3 can be estimated from Aspen Plus® for the given temperature and CO_2 loading. Figure 4.6 shows the heat of absorption of the solvent for a temperature range of 80 – 200°C.

The heat of absorption can also be calculated using Equations 3.17 – 3.18 as discussed in Section 3.2.2.4 with the input parameters of vapor pressure obtained from the flash calculation results.

$$Q_{desorption} = -\dot{m}_{CO_2} \, \Delta H_{absorption}$$

$$T_{max} = 120°C$$

$$P_{CO_2,lean}|_{T_{max}} = 19 \, kPa$$

$$P_{CO_2,lean}|_{40°C} = 1.6 \, kPa$$

$$R = 8.314 * 10^{-3} \, kJK^{-1}mol^{-1}$$

$$\Delta H_{absorption} = 31.6 \frac{kJ}{mol \, CO_2}$$

Mass flow rate of CO_2 in the absorber,

$$m_{CO_2}^{\cdot} = G_1 (y_1 - y_2)$$

$$m_{CO_2}^{\cdot} = 7.77 \frac{mol}{s} (0.0833 - 0.035) \frac{mol}{mol}$$

$$m_{CO_2}^{\cdot} = 0.37 \frac{mol}{s} = 0.011 \frac{kg}{s}$$

$$Q_{desorption} = 0.37 \frac{mol}{s} * 31.6 \frac{kJ}{mol\ CO_2} = 11.66\ kW$$

4.3.2. Sensible heat calculation

The specific heat of the solvent can be calculated from Aspen Plus® using a CPMX template in the NRTL method. At a rich CO_2 loading of 0.44 mol CO_2/mol K_2CO_3, the specific heat of solvent at 110°C is calculated as –

$$C_{p_{solvent,R}} = 3.02 \frac{kJ}{kg\ K}$$

The sensible heat in the regenerator can be calculated using equation 3.20.

$$Q_{sensible} = m_{solvent,R}^{\cdot}\ C_{p_{solvent,R}}\ \Delta T$$

$$Q_{sensible} = 1.14 \frac{kg}{s} * 3.02 \frac{kJ}{kg\ K} * 10°C$$

$$Q_{sensible} = 33.22\ kW$$

72

4.3.3. Calculation of heat of vaporization

From equation 3.21, we can calculate the heat of vaporization in the stripper. The partial pressure of CO_2 and H_2O can be estimated from the plot shown in Figure 4.2 and Figure 4.3 respectively.

$$Q_{vaporization} = \dot{m}_{CO_2} \frac{P_{H_2O} \; \Delta H_{vaporization,H_2O}}{P_{CO_2}}$$

$$Q_{vaporization} = 0.011 \frac{kg}{s} \frac{129 \; kPa * 2257 \frac{kJ}{kg}}{19 \; kPa}$$

$$Q_{vaporization} = 168.56 \; kW$$

4.3.4. Total Regeneration Energy

The total regeneration energy required in the stripper is given by –

$$Q_{reg} = Q_{desorption} + Q_{sensible} + Q_{vaporization}$$

$$Q_{reg} = 11.66 + 33.22 + 168.56 = 213.44 \; kW$$

As shown in the above calculations, the regeneration energy required for the CO_2 desorption process in the stripper is 213.44 kW at B50 operating point. This energy is dominated by the heat of vaporization of water in the stripper, therefore performance could be substantially improved by using a solvent with a higher heat of absorption and operating the system at higher temperature (both of which increase the ratio of water to CO_2 in the stripper). Similarly, we can calculate

73

the total regeneration energy required in the stripper for all the SET points from the flow rates of solvent obtained from the absorber calculations and the VLE behavior of the system. Table 4.2 shows the total regeneration energy in the stripper along with the mass flow rate of CO_2 for the SET points A25-C100.

Table 4.2. Total regeneration energy required for SET points A25-C100

SET Points	CO_2 (absorbed) Flow rate (kg/s)	Total Regeneration Energy (kW)
A25	0.005	98.41
A50	0.01	192.1
A75	0.014	270.25
A100	0.019	366.25
B25	0.006	118.21
B50	0.011	213.44
B75	0.016	312.34
B100	0.022	426.57
C25	0.007	137
C50	0.012	234.85

74

C75	0.017	332.51
C100	0.023	445.6

4.4. Results from GT-Suite® CO$_2$ Capture model

The heat exchangers, coolers and the condenser are modelled individually in GT-Suite® and are simulated before integrating these individual models to the CO$_2$ capture system model. In all the components, the heat exchanger specifications are kept same as that of a core air-air CAC for a large truck, shown in Table 3.4.

4.4.1. Results of Exhaust-absorbent heat exchanger

As illustrated in Section 3.2.3.1, the input parameters for the exhaust absorbent heat exchanger can be found in Table 3.2 and 3.3. The rich CO$_2$ solvent flow rate as well as the solvent composition is calculated in Section 4.2.2. From the theoretical calculations of the mass balance equation, the rich CO$_2$ solvent flow rate is estimated to be 1.14 kg/s. The heat rate obtained for the exhaust-absorbent heat exchanger for B50 operating point are shown in Table 4.3.

75

Table 4.3. GT-Post® results of exhaust-absorbent heat exchanger

Heat rejected by exhaust gas (kW)	73.1
Heat added to solvent (kW)	29.6

From Table 4.3, we see that at an outlet temperature of 40°C, 51.33 kW of heat is removed from the exhaust gas while 24.07 kW of heat is gained by the solvent at an outlet temperature of 120°C.

4.4.2. Results of Cross exchanger

The input parameters of the cross-exchanger model are shown in Table 3.5 and Table 3.6. The cross-exchanger transfers heat between the rich CO_2 solvent coming from the absorber and the lean CO_2 solvent coming from the stripper. The solvent flow rates with rich and lean CO_2 along with solvent composition is calculated. From the theoretical calculations of the mass balance equation, the solvent flow rate with lean CO_2 is estimated to be 1.12 kg/s. The results for the cross-exchanger are shown in Table 4.4.

Table 4.4. GT-Post® results of cross-exchanger

Heat gained by solvent stream with rich CO_2 loading (kW)	209.2
Heat rejected by solvent stream with lean CO_2 loading (kW)	163.3

4.4.3. Results of Trim cooler

Table 3.9 and 3.10 shows the input parameters of the trim cooler. The lean CO_2 solvent coming from the cross exchanger is cooled by water to maintain the desired temperature in the absorber. The lean CO_2 solvent flow rate and composition is calculated from absorber mass balance equation as shown in Section 4.2.2. The results for the trim cooler are shown in Table 4.5.

Table 4.5. GT-Post® results of trim cooler

Heat rejected by lean CO_2 solvent (kW)	31.2
Heat gained by water stream (kW)	19.6

4.4.4. Results obtained from condenser

The input parameters for the condenser can be obtained from Table 3.11 and Table 3.12. The vapor stream from the stripper/ flash comprising of CO_2 and H_2O is cooled by water at an initial temperature of 10°C. The water is drained, and the CO_2 is sent to the compressor. The CO_2 flow rate is calculated from the exhaust flow rate and CO_2 capture rate. The results obtained for the condenser with CO_2 stream is shown in Table 4.6.

Table 4.6. GT-Post® results of condenser with CO_2 stream

Heat rejected by CO_2 stream (kW)	1.02
Heat gained by water stream (kW)	2.6

The steam duty in the condenser or amount of heat rejected due to vaporization of water is calculated using equation 3.29.

$$Q_{H_2O} = m_{H_2O} \Delta H_{vaporization, H_2O}$$

$$Q_{H_2O} = 0.068 \frac{kg}{s} * 2257 \frac{kJ}{kg\ K} = 153.5\ kW$$

4.4.5. Work done by the compressor

The compressor work is calculated in GT-Suite® at a temperature of 120°C and an isentropic efficiency of 85% for a mid-speed, mid-load operating condition. To compress the CO_2 obtained from stripper to a desired pressure of 100 bar, the amount of work required is estimated as –

$$W_{compressor} = 19.5 \ kW$$

4.4.6. Energy Transfer across the system for SET points A25–C100.

The individual model of the heat exchangers, cooler and the condenser are then integrated into the CO_2 capture system model. The design specifications as well as the inlet and outlet temperatures are specified in the system. The solvent flow rates for rich and lean loading and their compositions are obtained from Table 4.1. Using a case setup, the exhaust gas parameters are varied accordingly for different operating conditions, from low-load to full-load along with their respective solvent flow rates and compositions, to obtain the energy transfer across the system. The model is then simulated for all the cases. Tables 4.7 and 4.8 shows the heat rate generated across the system while Table 4.9 shows the compressor work for different operating conditions from SET A25 (low-load) to C100 (full load).

79

Table 4.7. Heat rate generated in the exhaust-absorbent heat exchanger and trim cooler for SET operating points from A25 – C100.

SET data	Heat rejected by exhaust stream (kW)	Heat gained by solvent stream (kW)	Heat rejected by trim cooler (kW)
A25	36.3	16.3	11.7
A50	65.7	28.4	20
A75	97.5	40.3	29.2
A100	134.1	57.2	39
B25	45.6	19.6	17.5
B50	78.7	37.8	24.7
B75	113.7	49.1	36.1
B100	158.5	65.1	45.7
C25	52.1	22.2	15.9
C50	84.8	37.8	27.6
C75	122.2	52.9	38.1

80

SET data			
C100	169.4	69.3	48.4

Table 4.8. Heat rate generated in the cross exchanger and condenser for SET operating points from A25 – C100.

SET data	Heat rejected by solvent with lean loading (kW)	Heat gained by solvent with rich loading (kW)	Work done in condenser (kW)
A25	81.6	113.5	0.3
A50	143.8	197.6	0.8
A75	206.1	272.2	1.3
A100	272.6	364.5	2.1
B25	98.6	138	0.4
B50	181.3	231.4	0.9
B75	246.4	331.1	1.6
B100	328	435.4	2.6
C25	111.9	154.7	0.5

C50	194.3	255.7	1.0
C75	267.6	354.3	1.7
C100	342.8	452.8	2.8

Table 4.9. Work done by the compressor for SET operating points from A25 –

C100.

SET data	Work done by compressor (kW)
A25	4.23
A50	15.78
A75	28.18
A100	46.36
B25	5.27
B50	19.5
B75	36.56
B100	64.87

C25	7.65
C50	21.3
C75	41.45
C100	69.81

The total amount of work in the system is obtained by deducting the compressor work from engine power output as the power required for compressor is provided by other form of exhaust energy or waste heat recovery system. The engine output is obtained from the engine SET data. Table 4.10 shows the comparative analysis of the amount of CO_2 in the tailpipe after passing through the CO_2 absorber with 60% capture rate, per kW-hr with respect to net work for SET points A25-C100.

Table 4.10. Amount of CO_2 in tailpipe after 60% CO_2 absorption per kW-hr from the CO_2 capture system with respect to net work for SET points A25-C100.

SET Points	Tailpipe CO_2 Flow rate (kg/s)	Engine power output (kW)	Work done by compressor (kW)	Net work (kW)	Tailpipe CO_2 emissions (gCO_2/kW-hr)
A25	0.003	71.16	4.23	66.93	183.72
A50	0.006	142.51	15.78	126.73	181.27
A75	0.009	213.62	28.18	185.44	181.77
A100	0.013	284.98	46.36	238.62	190.64
B25	0.004	82.93	5.27	77.66	190.94
B50	0.008	166.01	19.5	146.51	184.54
B75	0.011	248.9	36.56	212.34	186.63
B100	0.015	331.85	64.87	266.98	199.63
C25	0.005	85.97	7.65	78.32	211.24
C50	0.008	171.98	21.3	150.68	193.28

84

C75	0.012	258.84	41.45	217.39	193.97
C100	0.015	341.76	69.81	271.95	203.47

According to EPA standards regulated under the GHG/CAFE vehicle regulations (2016), the CO_2 emissions standard for medium-duty engines are 772 g/kW-hr in 2017 and 731 g/kW-hr by 2021. For heavy-duty engines, the CO_2 emissions standard are 744 g/kW-hr in 2017 and 688 g/kW-hr by 2021.

85

Chapter 5

Conclusion and Recommendations

5.1. Conclusion

A CO_2 capture system is developed for a heavy-duty engine application. The system follows a thermal swing absorption process for CO_2 absorption at low temperature and desorption at high temperature. A series of heat exchangers and coolers are used to maintain the temperature requirement of the system.

A 40 wt.% K_2CO_3 solution is used as a solvent for the system due to its stability and non-volatile nature. The solvent regenerator is modelled using a flash drum in Aspen Plus which provides the CO_2 VLE data that helps determine the solvent flow rates, composition and other properties throughout the system by assuming a driving force for the mass transfer.

For a mid-speed, mid-load operating condition, the energy flow throughout the system involving heat rejected by exhaust gas, heat gained by the solvent stream and the regeneration energy produced due to CO_2 desorption is determined for a CO_2 absorption rate of 60% from the exhaust gas.

A model is developed in GT-Suite for the CO_2 capture system using HXMaster/Slave templates for heat exchangers and coolers and a 2D lookup table for the CO_2 stripper, with temperature and CO_2 loading as input and pressure as output. The heat exchangers, coolers and the condenser are modeled separately and sized for a mid-speed, mid-load operating condition and the solvent flow rates, water flow rates, outlet temperature and heat rate are determined. The outlet temperature and flow rate generated from results are set in the individual models before integrating it to the system model. The exhaust parameters such as temperature, pressure and composition are provided as input to the model for the mid-speed, mid-load operating condition. Assuming a 60% capture rate, the CO_2 flow rate is specified in the model. By keeping the design specifications, solvent flow rates and outlet temperature for the model constant, a case setup can be developed to calculate the heat transfer rate for the different SET operating conditions from idle to full load throughout the system.

5.2. Recommendations for future work

Future work on the CO_2 capture system can involve integrating the system to a waste heat recovery arrangement to fulfill the energy demand of the CO_2 capture system to a certain extent. The compressor in the CO_2 capture system can be coupled to the expander of an Organic Rankine Cycle (ORC), to provide the maximum cycle power output with a suitable refrigerant.

Experimental analysis of a CO_2 absorber and stripper can be performed to explore the tradeoffs and benefits of various solvents relative to K_2CO_3. Challenges involved like sizing the system for a heavy-duty engine can also be addressed.

Validating the model with experimental data from heat exchangers, coolers and condenser should also be performed.

References

[1] Benson et. al., *CO₂ absorption employing hot potassium carbonate solutions*. Chemical Engineering Prog., 1954. 50: p. 356 – 364.

[2] Chen, Xi, *Carbon Dioxide Thermodynamics, Kinetics, and Mass Transfer in Aqueous Piperazine Derivatives and Other Amines.* PhD Dissertation, The University of Texas at Austin, 2011.

[3] Cullinane, John T., *Thermodynamics and Kinetics of Aqueous Piperazine with Potassium Carbonate for Carbon Dioxide Absorption.* PhD Dissertation, The University of Texas at Austin, 2005.

[4] Dugas, Ross E., *Carbon Dioxide Absorption, Desorption, and Diffusion in Aqueous Piperazine and Monoethanolamine.* PhD Dissertation, The University of Texas at Austin, 2009.

[5] Gao, Shiwang, *Potassium Carbonate Slurry-Based CO2 Capture Technology.* ACS Energy Fuels, 2015, Vol. 29, p.6656-6663.

[6] Hilliard, Marcus D., *A Predictive Thermodynamic Model for an Aqueous Blend of Potassium Carbonate, Piperazine, and Monoethanolamine for Carbon Dioxide Capture from Flue Gas.* PhD Dissertation, The University of Texas at Austin, 2008.

[7] Hilliard, Marcus D., *Thermodynamics of Aqueous Piperazine/Potassium Carbonate/Carbon Dioxide Characterized by the Electrolyte NRTL Model within Aspen Plus®.* Topical Report, 2004.

[8] Kothandaraman Anusha, *Carbon Dioxide Capture by Chemical Absorption: A Solvent Comparison Study.* PhD Dissertation, Massachusetts Institute of Technology, 2010.

[9] Li, Le, *Carbon Dioxide Solubility and Mass Transfer in Aqueous Amines for Carbon Capture.* PhD Dissertation, The University of Texas at Austin, 2015.

[10] Li, Xiaofei, *Experimental study of energy requirement of CO2 desorption from rich solvent.* Energy Procedia 37, 2013, p.1836-1843.

[11] Mergler et. al., *Solvents for CO2 capture. Structure-activity relationships combined with Vapour-Liquid-Equilibrium measurements.* Energy Procedia 4, 2011, p.259-266.

[12] Tosh et. al., *Equilibrium study of the system Potassium Carbonate, Potassium Bicarbonate, Carbon Dioxide and Water.* 1959.

[13] Weiland et. al., *Density and Viscosity of Some Partially Carbonated Aqueous Alkanolamine Solutions and Their Blends.* Journal of Chemical and Engineering Data 1998, Vol. 43, p.378-382.

Appendix A

Table A.1. Total pressure from flash calculation in Aspen Plus as a function of Temperature and CO₂ loading

Temp(°C) Loading (mol CO$_2$ /mol (K$_2$CO$_3$)	Total Pressure (bar)												
	80	90	100	110	120	130	140	150	160	170	180	190	200
0	0.33	0.47	0.68	0.95	1.30	1.74	2.31	3.01	3.87	4.91	6.16	7.64	9.39
0.1	0.33	0.48	0.69	0.96	1.31	1.76	2.33	3.04	3.90	4.95	6.20	7.69	9.44
0.2	0.35	0.51	0.72	1.00	1.37	1.83	2.41	3.14	4.02	5.09	6.37	7.88	9.67
0.3	0.39	0.56	0.79	1.09	1.48	1.97	2.58	3.34	4.27	5.38	6.71	8.28	10.13
0.4	0.46	0.65	0.91	1.24	1.67	2.21	2.88	3.70	4.70	5.89	7.30	8.96	10.88
0.5	0.57	0.80	1.11	1.50	1.99	2.61	3.37	4.29	5.39	6.69	8.22	9.98	12.00
0.6	0.76	1.05	1.43	1.92	2.52	3.26	4.16	5.22	6.48	7.92	9.58	11.45	13.55
0.7	1.09	1.50	2.01	2.65	3.43	4.37	5.47	6.74	8.18	9.78	11.54	13.47	15.58
0.8	1.78	2.40	3.17	4.10	5.18	6.41	7.77	9.26	10.84	12.52	14.28	16.14	18.12
0.9	3.71	4.84	6.11	7.51	8.97	10.48	11.98	13.47	14.95	16.43	17.94	19.50	21.18
1	14.00	15.10	16.12	17.05	17.91	18.71	19.45	20.18	20.92	21.70	22.56	23.54	24.70

91

Table A.2. Partial Pressure of CO₂ from flash calculation in Aspen Plus as a function of Temperature and CO2 loading

Temp(°C) Loading (mol CO$_2$ /mol (K$_2$CO$_3$)						Partial Pressure of CO$_2$ (bar)							
	80	90	100	110	120	130	140	150	160	170	180	190	200
0	0.00	0.00	0.00	0.00	0.00	0.00	0.00	0.00	0.00	0.01	0.01	0.02	0.03
0.1	0.01	0.01	0.01	0.01	0.02	0.02	0.03	0.04	0.05	0.06	0.08	0.11	0.14
0.2	0.03	0.03	0.05	0.06	0.08	0.10	0.12	0.15	0.19	0.23	0.28	0.34	0.42
0.3	0.07	0.09	0.12	0.15	0.19	0.24	0.30	0.37	0.45	0.55	0.66	0.78	0.93
0.4	0.13	0.18	0.23	0.30	0.39	0.49	0.60	0.74	0.89	1.07	1.27	1.49	1.72
0.5	0.24	0.33	0.43	0.56	0.71	0.89	1.09	1.33	1.59	1.88	2.20	2.52	2.86
0.6	0.43	0.58	0.76	0.98	1.24	1.54	1.88	2.26	2.68	3.11	3.56	3.99	4.40
0.7	0.77	1.02	1.34	1.71	2.15	2.64	3.19	3.77	4.36	4.95	5.50	5.99	6.40
0.8	1.45	1.93	2.49	3.15	3.88	4.66	5.47	6.26	7.00	7.65	8.19	8.60	8.88
0.9	3.38	4.35	5.42	6.54	7.65	8.70	9.63	10.42	11.05	11.49	11.77	11.88	11.85
1	13.64	14.58	15.38	16.03	16.52	16.85	17.02	17.03	16.90	16.65	16.28	15.81	15.26

92

Table A.3. Partial Pressure of H_2O from flash calculation in Aspen Plus as a function of Temperature and CO_2 loading

Temp(°C) Loading (mol CO_2 /mol (K_2CO_3))	80	90	100	110	120	130	140	150	160	170	180	190	200
0	0.33	0.47	0.68	0.95	1.30	1.74	2.31	3.01	3.86	4.90	6.15	7.63	9.36
0.1	0.33	0.47	0.68	0.95	1.29	1.74	2.30	3.00	3.85	4.89	6.12	7.58	9.30
0.2	0.33	0.47	0.68	0.94	1.29	1.73	2.29	2.99	3.83	4.86	6.09	7.54	9.24
0.3	0.33	0.47	0.68	0.94	1.29	1.73	2.29	2.97	3.82	4.84	6.06	7.50	9.19
0.4	0.33	0.47	0.67	0.94	1.28	1.73	2.28	2.97	3.80	4.82	6.03	7.47	9.16
0.5	0.33	0.47	0.67	0.94	1.28	1.72	2.27	2.96	3.80	4.81	6.02	7.46	9.14
0.6	0.33	0.47	0.67	0.94	1.28	1.72	2.27	2.96	3.80	4.81	6.02	7.46	9.15
0.7	0.33	0.48	0.68	0.94	1.29	1.73	2.28	2.97	3.81	4.83	6.05	7.49	9.18
0.8	0.33	0.48	0.68	0.95	1.30	1.74	2.30	3.00	3.84	4.87	6.09	7.54	9.24
0.9	0.33	0.49	0.69	0.97	1.32	1.78	2.35	3.05	3.91	4.94	6.17	7.62	9.32
1	0.36	0.52	0.74	1.03	1.39	1.86	2.44	3.15	4.01	5.05	6.28	7.73	9.44

Partial Pressure of H_2O (bar)

93